

Impairments-Aware Resource Allocation for FD Massive MIMO Relay Networks: Sum Rate and Delivery-Time Optimization Perspectives

Vimal Radhakrishnan, *Member, IEEE*, Omid Taghizadeh, *Member, IEEE*, Rudolf Mathar, *Senior Member, IEEE*

Abstract—In this paper, we investigate the resource allocation problem for a full-duplex (FD) massive multiple input multiple output (mMIMO) multi-carrier (MC) decode and forward (DF) relay system which serves multiple MC single-antenna half-duplex (HD) nodes. In addition to the prior studies focusing on maximizing the sum-rate and energy efficiency, we focus on minimizing the overall delivery time for a given set of communication tasks to the user terminals. As our system is an FD MC system, we consider the impact of hardware distortions resulting in residual self-interference (SI) and inter-carrier leakage (ICL). We also consider that only limited channel state information (CSI) is available. A joint power and sub-carrier allocation problem to maximize the sum-rate of the system is then formulated. Due to the intractable nature of the underlying problem, an iterative solution is proposed, employing the successive inner approximation (SIA) framework, with guaranteed convergence to the point that satisfies the Karush–Kuhn–Tucker (KKT) conditions. For the energy efficiency maximization problem, a two-stage iterative algorithm which follows the SIA and Dinkelbach algorithm is proposed. The operation of an FD mMIMO MC DF relay system is evaluated for different system parameters using numerical simulations. We also show that the importance of considering delivery time minimization rather than the sum-rate maximization, i.e., maximizing the sum-rate of the system does not necessarily minimize the overall delivery time. Numerical results show the significance of distortion-aware design for such systems and also the significant gain in terms of different objectives such as sum-rate, energy efficiency, and delivery time compared to its HD counterpart.

I. INTRODUCTION

Multiple input multiple output (MIMO) relay has been widely studied as a practical approach to extend coverage as well as to improve spectral efficiency, especially at the cell edges [2]. Nevertheless, these systems require complex power allocation and precoder/decoder design. On the contrary, mMIMO relaying has received a substantial recognition over the past years, due to its ability to mitigate noise, inter-user interference and fast fading using simple linear processing [3]. Increasing the number of antennas reap all the benefits

of MIMO systems in terms of power and multiplexing gains. Moreover, large scale antennas provide more spatial degree of freedom that helps in better self-interference cancellation (SIC) [4]. Therefore, a relaying system with a large scale antenna array at the relay station appears to be a viable candidate to address the above-mentioned transceiver design challenges as well as to enable FD operation.

The spectral/energy efficiency of FD mMIMO relaying has been investigated in [5]–[10]. In [5], a power allocation scheme is proposed for FD mMIMO DF to maximize the energy efficiency for a given quality of service (sum spectral efficiency) under transmit power constraints. It is also shown that by increasing the number of transmit/receive antennas at the relay station, the transmit power at the source as well as the relay can be reduced. In [8], the authors demonstrate that, for an FD mMIMO DF relay system over Rician fading channels, the SI can be perfectly cancelled by zero-forcing (ZF) processing at the relay station without SI channel estimation when the number of antennas tends to infinity. However, the impact of hardware distortions is not taken into account in the above-mentioned works.

In [9], [10], the authors consider the FD mMIMO DF relaying system, where the FD relay is equipped with a large-scale antenna array simultaneously serve multiple source-destination pairs by taking into account the hardware impairments. In [9], an end-to-end achievable rate of the system is derived for the large-antenna regime by assuming MRT/MRC at the relay for single-antenna source-destination users. Furthermore, in [10], a hardware impairment aware transceiver scheme is proposed to cancel out the distortion noise for a more general model, where the source and destination are allowed to be equipped with multiple antennas. An asymptotic end-to-end achievable rate of the system with the proposed transceiver scheme is derived. However, the aforementioned works [9], [10] consider the hardware impairments in an FD mMIMO relay for a single carrier system.

Despite the aforementioned studies on the potential improvements achieved via FD mMIMO-enabled relaying systems, the impact of non-linear hardware impairments have not been addressed in the design and analysis of the related MC systems. Please note that for the FD mMIMO MC networks, the significance of the hardware impairments is two-fold [11]–[13]. Firstly, due to the large antenna array dimension, the utilization of low-cost components deteriorates the impairments characteristics of the transmit and receiver chains. The aforementioned effect is deteriorated for an FD-enabled transceiver, due to the strong SI channel. Secondly, the non-

V. Radhakrishnan and R. Mathar are with the Institute for Theoretical Information Technology, RWTH Aachen University, Aachen, 52074, Germany (email: {radhakrishnan, mathar}@ti.rwth-aachen.de).

O. Taghizadeh is with the Network Information Theory Group, Technische Universität Berlin, 10587 Berlin, Germany (email: {taghizadehmotlagh}@tu-berlin.de). This work has been supported by Deutsche Forschungsgemeinschaft (DFG), under the Grant No. MA 1184/38 – 1.

Part of this work has been presented in WSA 2020, 24nd International ITG Workshop on Smart Antennas [1].

linear hardware distortions spread over multiple subcarriers, leading to ICL¹. In particular, this calls for an impairments-aware design of the resource allocation strategies in the context of FD-mMIMO MC networks, which is the focus of this work.

A. Contribution and paper organization

In this paper, we consider the resource allocation problem for an FD mMIMO MC DF relay system, which serves multiple number of single-antenna source-destination pairs. The main contributions of this paper together with paper organizations are as follows:

- In Section II, the system model and the operation of the relay system by taking into account the hardware distortions leading to residual SI and ICL as well as the imperfect CSI are discussed. We extend the available frequency domain characterization of the distortion signals [12] for an orthogonal frequency division multiplexing (OFDM) system to a general MC system with orthogonal waveforms, e.g., orthogonal variable spreading factor (OVSF)-code division multiple access (CDMA) and the variations of orthogonal frequency division multiple access. Furthermore, we extend the employed modeling paradigm, relying on the linear dependency of the distortion variance to the desired signal variance, to a more general non-linear model. This is in contrast to the works in [5]–[10] where the impact of hardware impairments are ignored in the analysis of the multi-carrier systems, or to [11], [13] where the simplified linear model is used to predict the distortion statistics.
- Building on the obtained analysis, in Section III-C, we formulate joint sub-carrier and power allocation problems to maximize the overall weighted sum rate of the network, as well as to minimize the overall delivery time. The resulting mathematical problems are mathematically intractable, due to the non-convex rate expressions, as well as the inclusion of higher order dependencies describing the distortion signals. An iterative optimization solution is then proposed in each case, following the SIA framework, that converges to a point satisfying KKT optimality conditions.
- We also study the joint sub-carrier and power allocation problem to maximize the energy efficiency of the system. The resulting fractional optimization problem is then solved utilizing a dual-loop iterative algorithm, as a combination of the proposed SIA framework with the Dinkelbach's algorithm [14], converging to a KKT solution.

Extensive numerical simulations evaluate the impact of various source of impairments in the studied system, as well as the impact of different design strategies. In particular, the results show the significance of distortion-aware design for such systems and also the benefits of considering delivery time minimization rather than the sum-rate maximization, i.e., maximizing the sum-rate of the system does not necessarily minimize the overall delivery time.

¹This indicates that transmission at one subcarrier leads to the increased distortions effect over all subcarriers, i.e., ICL, due to its non-linear nature.

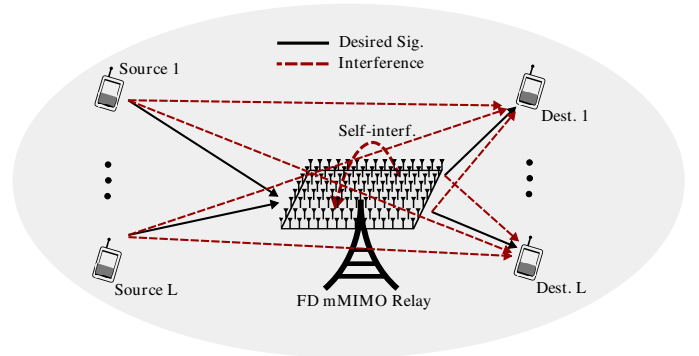


Fig. 1. Basic system model for FD mMIMO MC relay communication among L single-antenna source-destination pairs

B. Mathematical Notation

Throughout this paper, we denote the vectors and matrices by lower-case and upper-case bold letters, respectively. We use $\mathbb{E}\{\cdot\}$, $|\cdot|$, $\text{Tr}(\cdot)$, $(\cdot)^{-1}$, $(\cdot)^*$, $(\cdot)^T$, and $(\cdot)^H$ for mathematical expectation, determinant, trace, inverse, conjugate, transpose, and Hermitian transpose, respectively. We use $\text{diag}(\cdot)$ for the diag operator, which returns a diagonal matrix by setting off-diagonal elements to zero. We denote an all zero matrix of size $m \times n$ by $\mathbf{0}_{m \times n}$. We represent the Euclidean norm as $\|\cdot\|_2$. We denote the set of real, positive real and complex numbers as \mathbb{R} , \mathbb{R}^+ and \mathbb{C} , respectively. The function $\kappa(\mathbf{X}, \kappa^{(1)}, \kappa^{(2)}) := \kappa^{(1)}\mathbf{X} + \kappa^{(2)}\mathbf{X}^2$ is defined such that $\mathbf{X}, \kappa^{(1)}, \kappa^{(2)}$ are non-negative scalars or positive semi-definite diagonal matrices of the same size.

II. SYSTEM MODEL

We consider an MC DF relay setup, where L number of single-antenna HD source-destination pairs communicate through an mMIMO FD relay. The FD mMIMO relay consists of N antennas for both transmission and reception. Fig 1 presents a basic model for our system. We denote the index sets of all the source-destination pairs and sub-carriers by \mathbb{L} and \mathbb{K} respectively, where $|\mathbb{L}| = L$ and $|\mathbb{K}| = K$. Initially, the source nodes transmit signals to the relay through the source-relay channel. The desired source-relay channel from the i -th source to the relay using sub-carrier k can be represented as $\mathbf{h}_{\text{sr}}^{i,k} \in \mathbb{C}^{N \times 1}$. The signals received by the relay are decoded at the relay after employing SIC techniques. Then, the decoded signals are retransmitted to the destination nodes through the relay-destination channel. The $\mathbf{h}_{\text{rd}}^{i,k} \in \mathbb{C}^{1 \times N}$ represents desired relay-destination channel between the relay and the i -th destination node using the k -th sub-carrier. The SI channel at the relay can be denoted by $\mathbf{H}_{\text{tr}}^k \in \mathbb{C}^{N \times N}$. We consider weak signals, due to path loss, that are received at the destination nodes from source nodes to be interference, [11]. The direct channel between the source j and the destination i through the k -th sub-carrier can be represented as $h_{\text{sd}}^{i,j,k} \in \mathbb{C}^1$. We assume that all channels are constant for each frame and frequency flat in each carrier, please see Table I for a summary of the used notations.

TABLE I. LIST OF THE USED SYMBOLS IN THE DEFINED SYSTEM

Notation	Description
$\mathbf{H}_{\text{tr}}, \mathbf{h}_{\text{rd}}, \mathbf{h}_{\text{sd}}, \mathbf{h}_{\text{sr}}$	instantaneous flat-fading channel values
$\hat{\mathbf{H}}_{\text{tr}}, \hat{\mathbf{h}}_{\text{rd}}, \hat{\mathbf{h}}_{\text{sd}}, \hat{\mathbf{h}}_{\text{sr}}$	instantaneous flat-fading channel estimates
$\tilde{\mathbf{H}}_{\text{tr}}, \tilde{\mathbf{h}}_{\text{rd}}, \tilde{\mathbf{h}}_{\text{sd}}, \tilde{\mathbf{h}}_{\text{sr}}$	channel estimation error
$\mathbf{C}_{\text{tr}}^k, \mathbf{C}_{\text{rd}}^{i,k}, \mathbf{C}_{\text{sd}}^{i,j,k}, \mathbf{C}_{\text{sr}}$	channel estimation error covariance
$e_{\text{tx},s}, e_{\text{rx},r}, e_{\text{tx},r}, e_{\text{rx},d}$	additive distortion signals
$\kappa_l^{(1)}, \beta_l^{(1)}$	first-order transmit and receive distortion coefficients
$\kappa_l^{(2)}, \beta_l^{(2)}$	second-order transmit and receive distortion coefficients
p_s, p_r	transmit power from the source and relay
$\mathbf{v}_r, \mathbf{u}_r$	linear transmit and receive filters at the relay
$\sigma_{n,r}^2, \sigma_{n,d}^2$	thermal noise variance at the relay and destination
$\Sigma_r^{i,k}, \Sigma_d^{i,k}$	received total undesired sig. covariance
$\varphi_{r,i}, \varphi_{r,j}, \varphi_{s,i}, \varphi_{s,j}$	covariance of the total tx/rx signal at all subcarriers
$\mu_r^{i,k}, \mu_s^{i,k}$	effective desired channel variance
$\gamma_{r,i,j}, \gamma_{s,i,j}$	effective undesired chan. variance in source-relay link
$\bar{\gamma}_{s,i,j}, \bar{\gamma}_{r,i,j}$	effective undesired chan. variance in relay-dest. link
$R_{\text{sr}}^{i,k}, R_{\text{rd}}^{i,k}$	achievable rate

We consider a limited availability of CSI, i.e., only imperfect CSI of the channels are available. As in [15], the true channel, decomposed into the estimated channel and estimation error, can be represented as

$$\begin{aligned} \mathbf{h}_{\text{sr}}^{i,k} &= \hat{\mathbf{h}}_{\text{sr}}^{i,k} + \left(\mathbf{C}_{\text{sr}}^{i,k}\right)^{1/2} \tilde{\mathbf{h}}_{\text{sr}}^{i,k}, \quad \hat{\mathbf{h}}_{\text{sr}}^{i,k} \perp \tilde{\mathbf{h}}_{\text{sr}}^{i,k}, \\ \mathbf{h}_{\text{sd}}^{i,j,k} &= \hat{\mathbf{h}}_{\text{sd}}^{i,j,k} + \left(\mathbf{C}_{\text{sd}}^{i,j,k}\right)^{1/2} \tilde{\mathbf{h}}_{\text{sd}}^{i,j,k}, \quad \hat{\mathbf{h}}_{\text{sd}}^{i,j,k} \perp \tilde{\mathbf{h}}_{\text{sd}}^{i,j,k}, \\ \mathbf{h}_{\text{rd}}^{i,k} &= \hat{\mathbf{h}}_{\text{rd}}^{i,k} + \left(\mathbf{C}_{\text{rd}}^{i,k}\right)^{1/2} \tilde{\mathbf{h}}_{\text{rd}}^{i,k}, \quad \hat{\mathbf{h}}_{\text{rd}}^{i,k} \perp \tilde{\mathbf{h}}_{\text{rd}}^{i,k}, \end{aligned}$$

$\mathbf{H}_{\text{tr}}^k = \hat{\mathbf{H}}_{\text{tr}}^k + \left(\mathbf{C}_{\text{tr}}^k\right)^{1/2} \tilde{\mathbf{H}}_{\text{tr}}^k, \quad \hat{\mathbf{H}}_{\text{tr}}^k \perp \tilde{\mathbf{H}}_{\text{tr}}^k, \quad \forall i, j \in \mathbb{L}, \forall k \in \mathbb{K},$ (1) where the estimated channels of source-relay, source-destination, relay-destination, and relay SI channel can be represented as $\hat{\mathbf{h}}_{\text{sr}}^{i,k}, \hat{\mathbf{h}}_{\text{sd}}^{i,j,k}, \hat{\mathbf{h}}_{\text{rd}}^{i,k}$ and $\hat{\mathbf{H}}_{\text{tr}}^k$, respectively. The entries of channel estimation errors $\tilde{\mathbf{h}}_{\text{sr}}^{i,k}, \tilde{\mathbf{h}}_{\text{sd}}^{i,j,k}, \tilde{\mathbf{h}}_{\text{rd}}^{i,k}$ and $\tilde{\mathbf{H}}_{\text{tr}}^k$ are assumed to be independent and identically distributed (i.i.d.) complex Gaussian with zero mean and unit variance, where the correlation matrices $\mathbf{C}_{\text{sr}}^{i,k}, \mathbf{C}_{\text{sd}}^{i,j,k}, \mathbf{C}_{\text{rd}}^{i,k}$ and \mathbf{C}_{tr}^k shape the second-order statistics of the CSI error [11], [15], [16]. The statistical independence is obtained assuming that the receiver employs minimum mean squared error (MMSE) channel estimation strategy.

A. Source to Relay

The transmit signal from the i -th source node to the relay using the sub-carrier k can be written as

$$x_s^{i,k} = \sqrt{p_s^{i,k}} s_s^{i,k} + e_{t,s}^{i,k} = \tilde{x}_s^{i,k} + e_{t,s}^{i,k}, \quad i \in \mathbb{L}, \forall k \in \mathbb{K}, \quad (2)$$

where $s_s^{i,k} \in \mathbb{C}^1$ and $e_{t,s}^{i,k}$ represent the source symbol from the source i to the relay and transmit distortion at the i -th source node, respectively. We assume the source symbols are i.i.d. with unit power, i.e., $\mathbb{E}\{s_s^{i,k} (s_s^{i,k})^*\} = 1$. The intended transmit signal and transmit power at the i -th source node are denoted by $\tilde{x}_s^{i,k}$ and $p_s^{i,k}$.

Subsequently, the received signal at the relay from all the source nodes using the k -th sub-carrier can be stated as

$$\mathbf{y}_r^k = \sum_{i \in \mathbb{L}} \mathbf{h}_{\text{sr}}^{i,k} x_s^{i,k} + \mathbf{H}_{\text{tr}}^k \mathbf{x}_r + \mathbf{n}_r + \mathbf{e}_{\text{rx},r}^k = \tilde{\mathbf{y}}_r^k + \mathbf{e}_{\text{rx},r}^k, \quad (3)$$

where $\mathbf{n}_r^k \sim \mathcal{CN}(\mathbf{0}_N, (\sigma_{n,r}^k)^2 \mathbf{I}_N)$ and $\mathbf{e}_{\text{rx},r}^k$ represent the receiver noise and receive distortion at the relay, respectively. The transmitted signal and intended receive signal at the relay are defined as $\tilde{\mathbf{x}}_r^k$ and $\tilde{\mathbf{x}}_r^k$, respectively. Utilizing SIC techniques, the known part of SI can be removed from the received signal. However, the residual SI due to the CSI error and distortion remains in the system. Hence, the received signal after applying SIC can be obtained as

$$\tilde{\mathbf{y}}_r^k = \mathbf{y}_r^k - \hat{\mathbf{H}}_{\text{tr}}^k \tilde{\mathbf{x}}_r^k, \quad \forall k \in \mathbb{K}, \quad (4)$$

where $\tilde{\mathbf{x}}_r^k$ denotes the intended transmit signal at the relay. Correspondingly, the received signal from the i -th source at the relay after SIC can be written as

$$\tilde{\mathbf{y}}_r^{i,k} = \hat{\mathbf{h}}_{\text{sr}}^{i,k} \tilde{x}_s^{i,k} + \nu_r^{i,k}, \quad i \in \mathbb{L}, \forall k \in \mathbb{K}, \quad (5)$$

where the collective interference plus noise at the relay corresponding to the i -th source and the sub-carrier k can be defined as

$$\begin{aligned} \nu_r^{i,k} &:= \hat{\mathbf{h}}_{\text{sr}}^{i,k} e_{\text{tx},s}^{i,k} + \tilde{\mathbf{h}}_{\text{sr}}^{i,k} x_s^{i,k} + \sum_{\substack{j \in \mathbb{L} \\ j \neq i}} \mathbf{h}_{\text{sr}}^{j,k} x_s^{j,k} + \hat{\mathbf{H}}_{\text{tr}}^k \mathbf{e}_{\text{tx},r}^k \\ &\quad + \tilde{\mathbf{H}}_{\text{tr}}^k \mathbf{x}_r + \mathbf{n}_r + \mathbf{e}_{\text{rx},r}^k, \end{aligned}$$

where $\mathbf{e}_{\text{tx},r}^k$ represents the transmit distortion at the relay. The estimated received source symbol at the relay corresponding to the source i and sub-carrier k , considering $\mathbf{u}_r^{i,k} \in \mathbb{C}^{N \times 1}$ as the normalized linear receive filter, can be obtained as

$$\tilde{s}_s^{i,k} = (\mathbf{u}_r^{i,k})^H \tilde{\mathbf{y}}_r^{i,k}, \quad i \in \mathbb{L}, \quad \forall k \in \mathbb{K}. \quad (6)$$

B. Relay to Destination

The transmit signal from the relay to the destination nodes using sub-carrier k can be expressed as

$$\mathbf{x}_r^k = \sum_{i \in \mathbb{L}} \mathbf{v}_r^{i,k} \sqrt{p_r^{i,k}} s_r^{i,k} + \mathbf{e}_{\text{tx},r}^k = \tilde{\mathbf{x}}_r^k + \mathbf{e}_{\text{tx},r}^k, \quad \forall k \in \mathbb{K}, \quad (7)$$

where $s_r^{i,k} \in \mathbb{C}^1$, $p_r^{i,k}$ and $\mathbf{v}_r^{i,k} \in \mathbb{C}^{N \times 1}$ are the retransmitting source symbol, transmit power and normalized transmit precoder at the relay for the destination i utilizing sub-carrier k , respectively. We consider the source symbols to be i.i.d. with unit power ($\mathbb{E}\{s_r^{i,k} (s_r^{i,k})^*\} = 1$). Subsequently, the signal received at the destination i , including the interference from the source nodes, can be expressed as

$$y_d^{i,k} = \mathbf{h}_{\text{rd}}^{i,k} \mathbf{x}_r^k + \sum_{j \in \mathbb{L}} \mathbf{h}_{\text{sd}}^{i,j,k} x_s^{j,k} + n_d^{i,k} + e_{\text{rx},d}^{i,k} = \tilde{y}_d^{i,k} + e_{\text{rx},d}^{i,k}, \quad (8)$$

where the receive distortion and receiver noise at the i -th destination node are denoted by $e_{\text{rx},d}^{i,k}$ and $n_d^{i,k} \sim \mathcal{CN}(0, (\sigma_{n,d}^{i,k})^2)$, respectively. The intended receive signal at the destination i using sub-carrier k is defined as $\tilde{y}_d^{i,k}$. The above equation (8) can be rewritten as

$$y_d^{i,k} = \hat{\mathbf{h}}_{\text{rd}}^{i,k} \mathbf{v}_r^{i,k} \sqrt{p_r^{i,k}} s_r^{i,k} + \nu_d^{i,k}, \quad i \in \mathbb{L}, \forall k \in \mathbb{K}, \quad (9)$$

where the collective interference plus noise at the destination i can be defined as

$$\begin{aligned} \nu_d^{i,k} &:= \tilde{\mathbf{h}}_{\text{rd}}^{i,k} \mathbf{v}_r^{i,k} \sqrt{p_r^{i,k}} s_r^{i,k} + \sum_{\substack{j \in \mathbb{L} \\ j \neq i}} \mathbf{h}_{\text{rd}}^{i,k} \mathbf{v}_r^{j,k} \sqrt{p_r^{j,k}} s_r^{j,k} + \mathbf{h}_{\text{rd}}^{i,k} \mathbf{e}_{\text{tx},r}^k \\ &\quad + \sum_{j \in \mathbb{L}} \mathbf{h}_{\text{sd}}^{i,j,k} x_s^{j,k} + n_d^{i,k} + e_{\text{rx},d}^{i,k}, \quad i \in \mathbb{L}, \forall k \in \mathbb{K}. \end{aligned} \quad (10)$$

C. Hardware Distortions Statistics: Impact of Limited Dynamic Range

The inaccuracies of hardware components such as analog to digital/digital to analog converter error, noises caused by

$$\begin{aligned}
\Sigma_r^{i,k} \approx & \underbrace{\sum_{\substack{j \in \mathbb{L} \\ j \neq i}} \widehat{\mathbf{h}}_{\text{sr}}^{j,k} p_s^{j,k} (\widehat{\mathbf{h}}_{\text{sr}}^{j,k})^H}_{\text{Co-channel interference}} + \sum_{j \in \mathbb{L}} \mathbf{C}_{\text{sr}}^{j,k} p_s^{j,k} + \underbrace{\sum_{j \in \mathbb{L}} \widehat{\mathbf{h}}_{\text{sr}}^{j,k} \boldsymbol{\kappa} \left(\varphi_{s,j}(\mathbf{p}), \kappa_{s,j}^{(1)}, \kappa_{s,j}^{(2)} \right) (\widehat{\mathbf{h}}_{\text{sr}}^{j,k})^H}_{\text{Source transmit distortion}} + \sum_{j \in \mathbb{L}} \mathbf{C}_{\text{sr}}^{j,k} \boldsymbol{\kappa} \left(\varphi_{s,j}(\mathbf{p}), \kappa_{s,j}^{(1)}, \kappa_{s,j}^{(2)} \right) + \underbrace{(\sigma_{n,r}^k)^2 \mathbf{I}_N}_{\text{Thermal noise}} \\
& + \underbrace{\widehat{\mathbf{H}}_{\text{rr}}^k \boldsymbol{\kappa} \left(\varphi_{\text{rt}}(\mathbf{p}), \boldsymbol{\Theta}_{\text{t,r}}^{(1)}, \boldsymbol{\Theta}_{\text{t,r}}^{(2)} \right) (\widehat{\mathbf{H}}_{\text{rr}}^k)^H + \mathbf{C}_{e,\text{rr}}^k \text{Tr} \left(\boldsymbol{\kappa} \left(\varphi_{\text{rt}}(\mathbf{p}), \boldsymbol{\Theta}_{\text{t,r}}^{(1)}, \boldsymbol{\Theta}_{\text{t,r}}^{(2)} \right) \right)}_{\text{Relay transmit distortion}} + \underbrace{\boldsymbol{\kappa} \left(\varphi_{\text{r,r}}(\mathbf{p}), \boldsymbol{\Theta}_{\text{r,r}}^{(1)}, \boldsymbol{\Theta}_{\text{r,r}}^{(2)} \right)}_{\text{Relay receive distortion}} + \underbrace{\mathbf{C}_{\text{rr}}^k \text{Tr} \left(\sum_{j \in \mathbb{L}} \mathbf{v}_r^{j,k} p_r^{j,k} (\mathbf{v}_r^{j,k})^H \right)}_{\text{SI channel estimation error}}. \tag{11}
\end{aligned}$$

$$\begin{aligned}
\Sigma_d^{i,k} \approx & \underbrace{\widehat{\mathbf{h}}_{\text{rd}}^{i,k} \sum_{\substack{j \in \mathbb{L} \\ j \neq i}} \mathbf{v}_r^{j,k} p_r^{j,k} (\mathbf{v}_r^{j,k})^H (\widehat{\mathbf{h}}_{\text{rd}}^{i,k})^H + C_{\text{rd}}^{i,k} \text{Tr} \left(\sum_{j \in \mathbb{L}} \mathbf{v}_r^{j,k} p_r^{j,k} (\mathbf{v}_r^{j,k})^H \right)}_{\text{Co-channel interference}} + \underbrace{\sum_{j \in \mathbb{L}} \left(C_{\text{sd}}^{i,j,k} + |\widehat{h}_{\text{sd}}^{i,j,k}|^2 \right) \boldsymbol{\kappa} \left(\varphi_{s,j}(\mathbf{p}), \kappa_{s,j}^{(1)}, \kappa_{s,j}^{(2)} \right)}_{\text{Source transmit distortion}} + \underbrace{(\sigma_{n,d}^k)^2}_{\text{Thermal noise}} \\
& + \underbrace{\left(C_{\text{rd}}^{i,k} + \|\widehat{\mathbf{h}}_{\text{rd}}^{i,k}\|_2^2 \right) \boldsymbol{\kappa} \left(\varphi_{\text{rt}}(\mathbf{p}), \boldsymbol{\Theta}_{\text{t,r}}^{(1)}, \boldsymbol{\Theta}_{\text{t,r}}^{(2)} \right)}_{\text{Relay transmit distortion}} + \underbrace{\sum_{j \in \mathbb{L}} \left(\widehat{h}_{\text{sd}}^{i,j,k} p_s^{j,k} (\widehat{h}_{\text{sd}}^{i,j,k})^* + C_{\text{sd}}^{i,j,k} p_s^{j,k} \right)}_{\text{Direct channel interference}} + \underbrace{\boldsymbol{\kappa} \left(\varphi_{d,i}(\mathbf{p}), \kappa_{d,i}^{(1)}, \kappa_{d,i}^{(2)} \right)}_{\text{Destination receive distortion}}. \tag{12}
\end{aligned}$$

$$\varphi_{s,j}(\mathbf{p}) := \sum_{m \in \mathbb{K}} p_s^{j,m}, \quad \varphi_{\text{rt}}(\mathbf{p}) := \text{diag} \left(\sum_{j \in \mathbb{L}} \sum_{m \in \mathbb{K}} \mathbf{v}_r^{j,m} p_r^{j,m} (\mathbf{v}_r^{j,m})^H \right), \tag{13}$$

$$\varphi_{d,i}(\mathbf{p}) := \sum_{j \in \mathbb{L}} \sum_{m \in \mathbb{K}} \left(\widehat{\mathbf{h}}_{\text{rd}}^{i,m} \mathbf{v}_r^{j,m} p_r^{j,m} (\mathbf{v}_r^{j,m})^H (\widehat{\mathbf{h}}_{\text{rd}}^{i,m})^H + C_{\text{rd}}^{i,m} p_r^{j,m} + \widehat{h}_{\text{sd}}^{j,i,m} p_s^{j,m} (\widehat{h}_{\text{sd}}^{j,i,m})^* + C_{\text{sd}}^{j,i,m} p_s^{j,m} \right) + \sum_{m \in \mathbb{K}} (\sigma_{n,d}^m)^2 \tag{14}$$

$$\varphi_{\text{r,r}}(\mathbf{p}) := \sum_{m \in \mathbb{K}} \text{diag} \left(\sum_{j \in \mathbb{L}} \widehat{\mathbf{h}}_{\text{sr}}^{j,m} p_s^{j,m} (\widehat{\mathbf{h}}_{\text{sr}}^{j,m})^H + \sum_{j \in \mathbb{L}} \mathbf{C}_{\text{sr}}^{j,m} p_s^{j,m} + \widehat{\mathbf{H}}_{\text{rr}}^m \sum_{j \in \mathbb{L}} \mathbf{v}_r^{j,m} p_r^{j,m} (\mathbf{v}_r^{j,m})^H (\widehat{\mathbf{H}}_{\text{rr}}^m)^H + \mathbf{C}_{\text{rr}}^m p_r^{j,m} + (\sigma_{n,r}^m)^2 \mathbf{I}_N \right) \tag{15}$$

power amplifiers, automatic gain control and oscillator on transmit and receive chains are jointly modelled for FD MIMO transceiver in [11], [16], based on experimental results in [17]–[20], and used for the purpose of design and performance analysis of the FD-enabled systems, e.g., see [10], [21] and the references therein. The hardware inaccuracies of the transmit (receive) chain for each antenna is jointly modeled as an additive distortion, expressed as

$$\begin{aligned}
x_l(t) &= v_l(t) + e_{\text{tx},l}(t), \\
y_l(t) &= u_l(t) + e_{\text{rx},l}(t),
\end{aligned} \tag{16}$$

such that,

$$\begin{aligned}
e_{\text{tx},l}(t) &\sim \mathcal{CN} \left(0, \boldsymbol{\kappa} \left(\mathbb{E}\{|v_l(t)|^2\}, \kappa_l^{(1)}, \kappa_l^{(2)} \right) \right), \\
e_{\text{rx},l}(t) &\sim \mathcal{CN} \left(0, \boldsymbol{\kappa} \left(\mathbb{E}\{|u_l(t)|^2\}, \beta_l^{(1)}, \beta_l^{(2)} \right) \right),
\end{aligned} \tag{17}$$

$$e_{\text{tx},l}(t) \perp v_l(t), \quad e_{\text{tx},l}(t) \perp e_{\text{tx},l'}(t), \quad e_{\text{tx},l}(t) \perp e_{\text{tx},l}(t'), \tag{18}$$

$$\begin{aligned}
e_{\text{rx},l}(t) \perp u_l(t), \quad e_{\text{rx},l}(t) \perp e_{\text{rx},l'}(t), \quad e_{\text{rx},l}(t) \perp e_{\text{rx},l}(t'), \\
\forall t \neq t', \quad l \neq l',
\end{aligned} \tag{19}$$

which indicates the non-linear dependency of the variance of the additive distortion terms to the variance of the desired, i.e., undistorted, signal at the transmit and receiver chains. In the equations (16) and (17), t denotes the instance of time, and v_l (u_l), x_l (y_l) and $e_{\text{t},l}$ ($e_{\text{r},l}$) are respectively the baseband time-domain representation of the intended transmit (receive) signal, the actual transmit (receive) signal, and the additive transmit (receive) distortion at the l -th transmit (receive) chain. The coefficients $\kappa_l^{(1)}, \kappa_l^{(2)}$ ($\beta_l^{(1)}, \beta_l^{(2)}$) indicate the first and second order distortion coefficients at the transmitter (receiver) chains.

In [12], we discussed the characterization of the impact of these hardware distortions in the frequency domain for an OFDM system. In this paper, we extend this characterization in the frequency domain to a general MC strategy, where the sub-carriers k are orthogonal to each other with a unitary linear transformation, e.g., OVSA-CDMA, OFDM and cyclic-prefix (CP)-OFDM. Let \mathbf{Q} be a $K \times K$ unitary transformation matrix, where the columns of the matrix \mathbf{Q} represent the basis of the generalized sub-carrier waveforms which are orthonormal to each other. NT_s is the duration of one communication block, where T_s is the sample period. The unitary transformation representation of the sampled time domain signal for each communication block can be written as

$$\begin{aligned}
x_l^k &= \sum_{n=0}^{N-1} x_l(nT_s) q_{k,n}^* = \underbrace{\sum_{n=0}^{N-1} v_l(nT_s) q_{k,n}^*}_{=:v_l^k} + \underbrace{\sum_{n=0}^{N-1} e_{\text{tx},l}(nT_s) q_{k,n}^*}_{=:e_{\text{t},l}^k}, \\
y_l^k &= \sum_{n=0}^{N-1} y_l(nT_s) q_{k,n} = \underbrace{\sum_{n=0}^{N-1} u_l(nT_s) q_{k,n}^*}_{=:u_l^k} + \underbrace{\sum_{n=0}^{N-1} e_{\text{rx},l}(nT_s) q_{k,n}^*}_{=:e_{\text{r},l}^k},
\end{aligned} \tag{20}$$

where $q_{k,n}$ is the element of the unitary matrix \mathbf{Q} at the k -th row and the n -th column.

Lemma II.1. *Let us define \widetilde{x}_l^m and \widetilde{y}_l^m as the intended transmit and receive signal via m -th sub-carrier at the l -th transmit/receive chain. The impact of hardware distortions in the unitary transformed domain is characterized as*

$$R_{\text{sr}}^{i,k} = \gamma_0 \log_2 \left(1 + \frac{\mu_s^{i,k} p_s^{i,k}}{\alpha_{n,r}^{i,k} + \sum_{m \in \mathbb{K}} \sum_{j \in \mathbb{L}} (\gamma_{s,ij}^{km} p_s^{j,m} + \gamma_{r,ij}^{km} p_r^{j,m}) + \underbrace{\sum_{j \in \mathbb{L}} \bar{d}_{s,j}^{i,k} \varphi_{s,j}^2(\mathbf{p}) + \text{Tr}(\mathbf{D}_{r,r}^{i,k} \varphi_{r,r}^2(\mathbf{p})) + \text{Tr}(\mathbf{D}_{r,t}^{i,k} \varphi_{r,t}^2(\mathbf{p}))}_{=:\varphi_{\text{sr}}^{i,k}(\mathbf{p})}} \right), \quad (21)$$

$$R_{\text{rd}}^{i,k} = \gamma_0 \log_2 \left(1 + \frac{\mu_r^{i,k} p_r^{i,k}}{\alpha_{n,d}^{i,k} + \sum_{m \in \mathbb{K}} \sum_{j \in \mathbb{L}} (\bar{\gamma}_{s,ij}^{km} p_s^{j,m} + \bar{\gamma}_{r,ij}^{km} p_r^{j,m}) + \underbrace{\sum_{j \in \mathbb{L}} \bar{d}_{s,j}^{i,k} \varphi_{s,j}^2(\mathbf{p}) + \bar{d}_{d,i}^{i,k} \varphi_{d,i}^2(\mathbf{p}) + \text{Tr}(\bar{\mathbf{D}}_{r,t}^{i,k} \varphi_{r,t}^2(\mathbf{p}))}_{=:\varphi_{\text{rd}}^{i,k}(\mathbf{p})}} \right), \quad (22)$$

$$e_{t,l}^k \sim \mathcal{CN} \left(0, \kappa \left(\sum_{m=1}^K \mathbb{E} \{ |\tilde{y}_l^m|^2 \}, \tilde{\kappa}_l^{(1)}, \tilde{\kappa}_l^{(2)} \right) / K \right),$$

$$e_{\text{rx},l}^k \perp \tilde{y}_l^k, \quad e_{t,l}^k \perp e_{r,l'}^k, \quad (23)$$

$$e_{r,l}^k \sim \mathcal{CN} \left(0, \kappa \left(\sum_{m=1}^K \mathbb{E} \{ |\tilde{x}_l^m|^2 \}, \tilde{\beta}_l^{(1)}, \tilde{\beta}_l^{(2)} \right) / K \right),$$

$$e_{\text{rx},l}^k \perp \tilde{x}_l^k, \quad e_{r,l}^k \perp e_{r,l'}^k, \quad (24)$$

transforming the statistical independence, as well as the proportional variance properties from the time domain. Here, K represents the total number of sub-carriers. The scalars $\tilde{\kappa}_l^{(1)}, \tilde{\kappa}_l^{(2)}$ ($\tilde{\beta}_l^{(1)}, \tilde{\beta}_l^{(2)}$) respectively correspond to the first and second order transmit (receive) distortion coefficients at the l -th transmit (receive) chain.

Proof: Please refer to the Appendix. ■

Following the Lemma II.1, the statistics of the distortion terms can be obtained as

$$e_{\text{tx},s}^{i,k} \sim \mathcal{CN} \left(0, \kappa \left(\sum_{k \in \mathbb{K}} \mathbb{E} \{ \tilde{x}_s^{i,k} (\tilde{x}_s^{i,k})^H \}, \tilde{\kappa}_{s,i}^{(1)}, \tilde{\kappa}_{s,i}^{(2)} \right) / K \right),$$

$$e_{\text{tx},r}^k \sim \mathcal{CN} \left(\mathbf{0}_N, \kappa \left(\sum_{k \in \mathbb{K}} \text{diag} \left(\mathbb{E} \{ \tilde{\mathbf{x}}_r^k (\tilde{\mathbf{x}}_r^k)^H \} \right), \tilde{\Theta}_{t,r}^{(1)}, \tilde{\Theta}_{t,r}^{(2)} \right) / K \right),$$

$$e_{r,r}^k \sim \mathcal{CN} \left(\mathbf{0}_N, \kappa \left(\sum_{k \in \mathbb{K}} \text{diag} \left(\mathbb{E} \{ \tilde{\mathbf{y}}_r^k (\tilde{\mathbf{y}}_r^k)^H \} \right), \tilde{\Theta}_{r,r}^{(1)}, \tilde{\Theta}_{r,r}^{(2)} \right) / K \right),$$

$$e_{r,d}^{i,k} \sim \mathcal{CN} \left(0, \kappa \left(\sum_{k \in \mathbb{K}} \mathbb{E} \{ \tilde{y}_d^{i,k} (\tilde{y}_d^{i,k})^H \}, \tilde{\beta}_{d,i}^{(1)}, \tilde{\beta}_{d,i}^{(2)} \right) / K \right), \quad (25)$$

where the first and second order transmit (receive) distortion coefficients of the i -th source (destination) node can be respectively denoted as $\tilde{\kappa}_{s,i}^{(1)}, \tilde{\kappa}_{s,i}^{(2)}$ ($\tilde{\beta}_{d,i}^{(1)}, \tilde{\beta}_{d,i}^{(2)}$). The diagonal matrices $\tilde{\Theta}_{t,r}^{(1)}, \tilde{\Theta}_{t,r}^{(2)}$ and $\tilde{\Theta}_{r,r}^{(1)}, \tilde{\Theta}_{r,r}^{(2)}$ consist of first and second order transmit and receive distortion coefficients for the corresponding chains at the mMIMO relay, respectively. In order to simplify further calculations, we define $\kappa_{s,i}^{(\ell)} = \frac{\tilde{\kappa}_{s,i}^{(\ell)}}{K}$,

$$\beta_{d,i}^{(\ell)} = \frac{\tilde{\beta}_{d,i}^{(\ell)}}{K}, \quad \Theta_{t,r}^{(\ell)} = \frac{1}{K} \tilde{\Theta}_{t,r}^{(\ell)}, \quad \text{and} \quad \Theta_{r,r}^{(\ell)} = \frac{1}{K} \tilde{\Theta}_{r,r}^{(\ell)}.$$

By employing Lemma II.1, and equation (25) on (II-A), the covariance of received collective interference-plus-noise signal at the relay corresponding to the i -th source node and sub-carrier k can be expressed as in (11), where \mathbf{p} is the vector consisting of all transmit power variables in the network, and $\varphi_{s,j}(\mathbf{p}), \varphi_{d,j}(\mathbf{p})$ respectively represent the

collective transmitted signal power from the source and the collective received signal power at the destination. Similarly, the functions $\varphi_{r,r}(\mathbf{p}), \varphi_{r,t}(\mathbf{p})$ respectively represent the diagonalized collective transmit and received signal covariance at the relay. In the derivation of (11) we utilize the fact that the variance of the distortion signal is much smaller compared to the variance of desired, i.e., undistorted signal, at the corresponding chain, i.e., $\kappa(x, \kappa^{(1)}, \kappa^{(2)}) \ll x$, for all chains [11], [15], [16]. Similarly, the covariance of the received collective interference-plus-noise signal for sub-carrier k at the i -th destination node can be calculated as in (12).

D. Achievable Information Rate

In this section, we analyze the achievable information rate of our system under hardware impairments. The achievable information rate between the relay and the i -th source node using the k -th sub-carrier can be obtained as (21), where

$$\mu_s^{i,k} = |(\mathbf{u}_r^{i,k})^H \hat{\mathbf{h}}_{\text{sr}}^{i,k}|^2,$$

$$\gamma_{s,ij}^{km} = \delta_{km} (1 - \delta_{ij}) (\mathbf{u}_r^{i,k})^H \hat{\mathbf{h}}_{\text{sr}}^{j,k} (\hat{\mathbf{h}}_{\text{sr}}^{j,k})^H \mathbf{u}_r^{i,k} + \delta_{km} (\mathbf{u}_r^{i,k})^H \mathbf{C}_{e,\text{sr}}^{j,k} \mathbf{u}_r^{i,k}$$

$$+ (\mathbf{u}_r^{i,k})^H \hat{\mathbf{h}}_{\text{sr}}^{j,k} \kappa_{s,j}^{(1)} (\hat{\mathbf{h}}_{\text{sr}}^{j,k})^H \mathbf{u}_r^{i,k} + \kappa_{s,j}^{(1)} (\mathbf{u}_r^{i,k})^H \mathbf{C}_{e,\text{sr}}^{j,k} \mathbf{u}_r^{i,k}$$

$$+ (\mathbf{u}_r^{i,k})^H \Theta_{r,r}^{(1)} \left(\text{diag} \left(\hat{\mathbf{h}}_{\text{sr}}^{j,m} (\hat{\mathbf{h}}_{\text{sr}}^{j,m})^H \right) + \mathbf{C}_{\text{sr}}^{j,m} \right) \mathbf{u}_r^{i,k},$$

$$\gamma_{r,ij}^{km} = (\mathbf{u}_r^{i,k})^H \hat{\mathbf{H}}_{\text{tr}}^{(1)} \Theta_{t,r}^{(1)} \text{diag} \left(\mathbf{v}_r^{j,m} (\mathbf{v}_r^{j,m})^H \right) (\hat{\mathbf{H}}_{\text{tr}}^m)^H \mathbf{u}_r^{i,k}$$

$$+ (\mathbf{u}_r^{i,k})^H \left((\delta_{km} \mathbf{I}_N + \text{Tr} \left(\Theta_{t,r}^{(1)} \text{diag} \left(\mathbf{v}_r^{j,m} (\mathbf{v}_r^{j,m})^H \right) \right) \right) \mathbf{C}_{\text{tr}}^k \mathbf{u}_r^{i,k}$$

$$+ (\mathbf{u}_r^{i,k})^H \Theta_{r,r}^{(1)} \left(\text{diag} \left(\hat{\mathbf{H}}_{\text{tr}}^m \mathbf{v}_r^{j,m} (\mathbf{v}_r^{j,m})^H (\hat{\mathbf{H}}_{\text{tr}}^m)^H \right) + \mathbf{C}_{\text{tr}}^m \right) \mathbf{u}_r^{i,k},$$

$$d_{s,j}^{i,k} = (\mathbf{u}_r^{i,k})^H \hat{\mathbf{h}}_{\text{sr}}^{j,k} \kappa_{s,j}^{(2)} (\hat{\mathbf{h}}_{\text{sr}}^{j,k})^H \mathbf{u}_r^{i,k} + \kappa_{s,j}^{(2)} (\mathbf{u}_r^{i,k})^H \mathbf{C}_{\text{sr}}^{j,k} \mathbf{u}_r^{i,k},$$

$$\mathbf{D}_{r,t}^{i,k} = \Theta_{t,r}^{(2)} \left((\hat{\mathbf{H}}_{\text{tr}}^m)^H \mathbf{u}_r^{i,k} (\mathbf{u}_r^{i,k})^H \hat{\mathbf{H}}_{\text{tr}}^m + \text{Tr} \left(\mathbf{u}_r^{i,k} (\mathbf{u}_r^{i,k})^H \mathbf{C}_{\text{tr}}^k \right) \right) \mathbf{I}_N$$

$$\mathbf{D}_{r,r}^{i,k} = \mathbf{u}_r^{i,k} (\mathbf{u}_r^{i,k})^H \Theta_{r,r}^{(2)},$$

$$\alpha_{n,r}^{i,k} = (\mathbf{u}_r^{i,k})^H \left(\Theta_{r,r}^{(1)} \sum_{m \in \mathbb{K}} (\sigma_{n,r}^m)^2 \mathbf{I}_N + (\sigma_{n,r}^k)^2 \mathbf{I}_N \right) \mathbf{u}_r^{i,k}$$

and $\gamma_0 = (T_{\text{tot}} - T_{\text{train}}) / T_{\text{tot}}$ represents the fraction of time interval allocated for the data transmission. The channel coherence time interval and channel estimation (training) time interval are denoted by T_{tot} and T_{train} , respectively. Subsequently, the achievable information rate between the relay and the i -th destination node using the k -th sub-carrier can be obtained as (22), where $\mu_r^{i,k} = |\hat{\mathbf{h}}_{\text{rd}}^{i,k} \mathbf{v}_r^{i,k}|^2$,

$$\bar{\gamma}_{s,ij}^{km} = \delta_{km} \hat{h}_{\text{sd}}^{i,j,k} (\hat{h}_{\text{sd}}^{i,j,k})^* + \delta_{km} C_{\text{sd}}^{i,j,k} + \hat{h}_{\text{sd}}^{i,j,k} \kappa_{s,j}^{(1)} (\hat{h}_{\text{sd}}^{i,j,k})^*$$

$$+ C_{\text{sd}}^{i,j,k} \kappa_{s,j}^{(1)} + \beta_{d,i}^{(1)} \left(\hat{h}_{\text{sd}}^{i,j,m} (\hat{h}_{\text{sd}}^{i,j,m})^H + C_{\text{sd}}^{i,j,m} \right),$$

$$\begin{aligned} \bar{\gamma}_{r,i}^{km} &= \delta_{km} (1 - \delta_{ij}) \widehat{\mathbf{h}}_{rd}^{i,k} \mathbf{v}_r^{j,k} (\mathbf{v}_r^{j,k})^H (\widehat{\mathbf{h}}_{rd}^{i,k})^H + \delta_{km} C_{rd}^{i,k} \\ &+ \widehat{\mathbf{h}}_{rd}^{i,k} \Theta_{t,r}^{(1)} \text{diag} \left(\mathbf{v}_r^{j,m} (\mathbf{v}_r^{j,m})^H \right) (\widehat{\mathbf{h}}_{rd}^{i,k})^H \\ &+ C_{rd}^{i,k} \text{Tr} \left(\Theta_{t,r}^{(1)} \text{diag} \left(\mathbf{v}_r^{j,m} (\mathbf{v}_r^{j,m})^H \right) \right) \\ &+ \beta_{d,i}^{(1)} \left(\widehat{\mathbf{h}}_{rd}^{i,m} \mathbf{v}_r^{j,m} (\mathbf{v}_r^{j,m})^H (\widehat{\mathbf{h}}_{rd}^{i,m})^H + C_{rd}^{i,m} \right), \end{aligned}$$

$$\begin{aligned} \bar{d}_{s,j}^{i,k} &= \widehat{h}_{sd}^{i,j,k} \kappa_{s,j}^{(2)} (\widehat{h}_{sd}^{i,j,k})^* + C_{sd}^{i,j,k} \kappa_{s,j}^{(2)}, \\ \bar{\mathbf{D}}_{r,t}^{i,k} &= \left((\widehat{\mathbf{h}}_{rd}^{i,k})^H \widehat{\mathbf{h}}_{rd}^{i,k} + C_{rd}^{i,k} \mathbf{I}_N \right) \Theta_{t,r}^{(2)}, \quad \bar{d}_d^{i,k} = \beta_{d,i}^{(2)}, \end{aligned}$$

and $\alpha_{n,d}^{i,k} = \beta_{d,i}^{(1)} \sum_{m \in \mathbb{K}} (\sigma_{n,d}^{i,m})^2 + (\sigma_{n,d}^{i,k})^2$. Since the relay is equipped with a large antenna array, well-studied linear beamforming and precoding techniques such as MRT/MRC, ZF and MMSE can be considered as relay precoder-decoder strategies.

The total achievable information rate for the i -th source-destination pair using the k -th sub-carrier can be written as

$$R_{sr}^{i,k} = \min\{R_{sr}^{i,k}, R_{rd}^{i,k}\}. \quad (26)$$

Please note that the above analysis holds true for any statistics of the instantaneous channel, number of antenna, as well as the linear transmit and receive filter. In an asymptotically large antenna regime, the calculation of the above coefficients will incur a significant computational overhead. However, when the statistics of the instantaneous channel values are known, the calculations can be well approximated in the asymptotic region with minimal computational overhead, see, e.g., [22] where such computations are facilitated for a simpler system setup.

III. JOINT SUBCARRIER AND POWER ALLOCATION FOR MMIMO FD MC RELAY

In this section, we formulate the joint sub-carrier and power allocation optimization problem for FD mMIMO DF relay system. We incorporate the sub-carrier allocation into the power allocation problem such that if the power allocated to a particular sub-carrier associated with the source/destination node is zero, then the node is not transmitting or receiving in that sub-carrier. Three optimization problems namely weighted sum-rate maximization, energy efficiency maximization, and delivery time minimization, are considered in the following.

A. Weighted Sum Rate Maximization

The sum-rate maximization problem under transmit power constraints for an FD mMIMO DF relay system can be formulated as

$$\max_{\{p_s^{i,k}\}, \{p_r^{i,k}\}} \sum_{i \in \mathbb{L}} w_i \sum_{k \in \mathbb{K}} R^{i,k}(\mathbf{p}) \quad (27a)$$

$$\text{s.t.} \quad \sum_{i \in \mathbb{L}} \sum_{k \in \mathbb{K}} p_r^{i,k} \leq p_r, \quad \sum_{k \in \mathbb{K}} p_s^{i,k} \leq p_s^i, \quad i \in \mathbb{L}, \quad (27b)$$

$$p_s^{i,k} \geq 0, \quad p_r^{i,k} \geq 0, \quad \forall i \in \mathbb{L}, k \in \mathbb{K}, \quad (27c)$$

where p_s^i and p_r are the maximum available transmit power at the i -th source node and the relay, respectively. The weight corresponding to the user i is denoted by w_i , representing the significance of the requested service. The above problem can

be written in its epigraph form as

$$\max_{\{p_s^{i,k}\}, \{p_r^{i,k}\}, t} t \quad (28a)$$

$$\text{s.t.} \quad \sum_{i \in \mathbb{L}} w_i \sum_{k \in \mathbb{K}} R_{sr}^{i,k} \geq t, \quad (28b)$$

$$\sum_{i \in \mathbb{L}} w_i \sum_{k \in \mathbb{K}} R_{rd}^{i,k} \geq t, \quad (28c)$$

$$(27b), (27c). \quad (28d)$$

Unfortunately, the above problem is not tractable in the current form due to the non-convex rate expressions in the objective. In order to obtain a more tractable form, we equivalently formulate the above problem as

$$\max_{\{p_s^{i,k}\}, \{p_r^{i,k}\}, \{\zeta_{sr}^{i,k}, \zeta_{rd}^{i,k}\}, t} t \quad (29a)$$

$$\text{s.t.} \quad \sum_{i \in \mathbb{L}} w_i \sum_{k \in \mathbb{K}} R_{sr}^{i,k}(\mathbf{p}, \zeta_{sr}^{i,k}) \geq t, \quad (29b)$$

$$\sum_{i \in \mathbb{L}} w_i \sum_{k \in \mathbb{K}} R_{rd}^{i,k}(\mathbf{p}, \zeta_{rd}^{i,k}) \geq t, \quad (29c)$$

$$\varphi_{rd}^{i,k}(\mathbf{p}) = \zeta_{rd}^{i,k}, \quad \varphi_{sr}^{i,k}(\mathbf{p}) = \zeta_{sr}^{i,k}, \quad (29d)$$

$$(27b), (27c), \quad (29e)$$

where $R_{sr}^{i,k}(\mathbf{p}, \zeta_{sr}^{i,k})$, similar to $R_{rd}^{i,k}(\mathbf{p}, \zeta_{rd}^{i,k})$, is constructed by replacing the part of the denominator $R_{sr}^{i,k}(\mathbf{p})$ represented as $\varphi_{sr}^{i,k}(\mathbf{p})$ by $\zeta_{sr}^{i,k}$. Please note that the constraint (29d) is a tight non-convex constraint in the current form. In order to convexify the constraints in (29d), the relaxed version of the above problem is formulated as

$$\max_{\{p_s^{i,k}\}, \{p_r^{i,k}\}, \{\zeta_{sr}^{i,k}, \zeta_{rd}^{i,k}\}, t} t \quad (30a)$$

$$\text{s.t.} \quad \varphi_{rd}^{i,k}(\mathbf{p}) \leq \zeta_{rd}^{i,k}, \quad \varphi_{sr}^{i,k}(\mathbf{p}) \leq \zeta_{sr}^{i,k}, \quad (30b)$$

$$(27b), (27c), (29b), (29c), \quad (30c)$$

where the constraints in (30b) now constitute a convex set, due to the convex quadratic nature of the functions $\varphi_{rd}^{i,k}(\mathbf{p}), \varphi_{sr}^{i,k}(\mathbf{p})$ over \mathbf{p} . The following lemma presents the tightness of the utilized relaxation:

Lemma III.1. *Let the variable set $\mathbf{p}^*, \{\zeta_{sr}^{i,k*}, \zeta_{rd}^{i,k*}\}$ belong to the optimum solution set for the relaxed problem (30). Then we have:*

$$\varphi_{rd}^{i,k}(\mathbf{p}^*) = \zeta_{rd}^{i,k*}, \quad \varphi_{sr}^{i,k}(\mathbf{p}^*) = \zeta_{sr}^{i,k*}, \quad (31)$$

indicating the tightness of the constraints (30b) at the optimality.

Proof: The proof is obtained via contradiction, assuming one of the relaxed constraints is not tight at the optimality, e.g., $\varphi_{rd}^{i,k}(\mathbf{p}^*) < \zeta_{rd}^{i,k*}$. This indicates that there exist a feasible $\zeta_{rd}^{i,k}$, for which $\zeta_{rd}^{i,k} < \zeta_{rd}^{i,k*}$. Since the rate functions are monotonically decreasing in the value of $\zeta_{rd}^{i,k}$, it directly means that the feasible value $\zeta_{rd}^{i,k}$ is superior than $\zeta_{rd}^{i,k*}$ in terms of the resulting system sum rate. This contradicts the optimality assumption of $\mathbf{p}^*, \{\zeta_{sr}^{i,k*}, \zeta_{rd}^{i,k*}\}$, which concludes the proof. ■

The above lemma establishes the equivalence of the relaxed problem (30) with (28) and consequently with (27) at the optimality. Please note that the relaxed optimization problem (30) is still a non-convex problem, due to the rate expressions (29b), (29c). Nevertheless, it belongs to the class of smooth

difference of convex (DC) optimization problems, which can be iteratively solved following the SIA framework presented in [23], by iteratively approximate the problem (30) as a convex subproblem. In order to implement this, let us first select a feasible variable set $\mathbf{p}_0, \{\zeta_{\text{sr},0}^{i,k}, \zeta_{\text{rd},0}^{i,k}\}$. By recalling the DC nature of the rate expressions, following the proposed framework in [23], we construct a lower bound on the rate expressions as

$$\begin{aligned} & R_{\text{sr}}^{i,k}(\mathbf{p}, \zeta_{\text{sr}}^{i,k}) \geq \\ & \gamma_0 \log_2 \left(\alpha_{\text{n,r}}^{i,k} + \zeta_{\text{sr}}^{i,k} + \sum_{m \in \mathbb{K}} \sum_{j \in \mathbb{L}} (\gamma_{s,ij}^{km} p_s^{j,m} + \gamma_{r,ij}^{km} p_r^{j,m}) + \mu_s^{i,k} p_s^{i,k} \right) \\ & - \gamma_0 \log_2 \left(\alpha_{\text{n,r}}^{i,k} + \zeta_{\text{sr},0}^{i,k} + \sum_{m \in \mathbb{K}} \sum_{j \in \mathbb{L}} (\gamma_{s,ij}^{km} p_{s,0}^{j,m} + \gamma_{r,ij}^{km} p_{r,0}^{j,m}) \right) \\ & - \frac{\gamma_0 \sum_{m \in \mathbb{K}} \sum_{j \in \mathbb{L}} (\gamma_{s,ij}^{km} (p_s^{j,m} - p_{s,0}^{j,m}) + \gamma_{r,ij}^{km} (p_r^{j,m} - p_{r,0}^{j,m}) + \zeta_{\text{sr}}^{i,k} - \zeta_{\text{sr},0}^{i,k})}{\log(2) \left(\alpha_{\text{n,r}}^{i,k} + \zeta_{\text{sr},0}^{i,k} + \sum_{m \in \mathbb{K}} \sum_{j \in \mathbb{L}} (\gamma_{s,ij}^{km} p_{s,0}^{j,m} + \gamma_{r,ij}^{km} p_{r,0}^{j,m}) \right)} \\ & =: \bar{R}_{\text{sr}}^{i,k}(\mathbf{p}, \zeta_{\text{sr}}^{i,k}), \end{aligned} \quad (32)$$

where $\bar{R}_{\text{sr}}^{i,k}$ is obtained by employing the Taylor's approximation on the concave terms included in the rate expressions, leading to a smooth and locally tight lower bound for the rate expressions $R_{\text{sr}}^{i,k}$ [24].

Similarly, by applying first order Taylor's approximation on $R_{\text{rd}}^{i,k}$, we can obtain the lower bound as $\bar{R}_{\text{rd}}^{i,k}$. Using this approximation, we can write $\bar{R}^{i,k} = \min\{\bar{R}_{\text{sr}}^{i,k}, \bar{R}_{\text{rd}}^{i,k}\}$, which is a jointly concave function over $p_s^{i,k}$ and $p_r^{i,k}$. At each iteration of the optimization steps the approximated optimization problem is hence formulated as

$$\max_{\{p_s^{i,k}\}, \{p_r^{i,k}\}, \{\zeta_{\text{sr}}^{i,k}, \zeta_{\text{rd}}^{i,k}\}, t} \quad t \quad (33a)$$

$$\text{s.t.} \quad \sum_{i \in \mathbb{L}} w_i \sum_{k \in \mathbb{K}} \bar{R}_{\text{sr}}^{i,k}(\mathbf{p}, \zeta_{\text{sr}}^{i,k}) \geq t, \quad (33b)$$

$$\sum_{i \in \mathbb{L}} w_i \sum_{k \in \mathbb{K}} \bar{R}_{\text{rd}}^{i,k}(\mathbf{p}, \zeta_{\text{rd}}^{i,k}) \geq t, \quad (33c)$$

$$\varphi_{\text{rd}}^{i,k}(\mathbf{p}) \leq \zeta_{\text{rd}}^{i,k}, \quad \varphi_{\text{sr}}^{i,k}(\mathbf{p}) \leq \zeta_{\text{sr}}^{i,k}, \quad (33d)$$

$$(27b), (27c), \quad (33e)$$

which is a convex optimization problem and can be solved via standard numerical solvers [24]. The proposed iterative update is continued until a stable point is reached. Since we use a first-order Taylor approximation on a smooth convex function, we can conclude that $\bar{R}^{i,k}$ represents a global and tight lower bound to $R^{i,k}$, with a shared slope at the point of approximation [24]. As a result, the proposed iterative update also fulfills the requirements set in [23, Theorem 1], and hence converges to a point that satisfies KKT optimality conditions. Algorithm 1 defines the detailed algorithm procedure.

B. Energy Efficiency Maximization

In this section, the energy efficiency is defined as the ratio of the sum-rate to the total power consumption of all the user nodes and the relay. The total power consumption P_{tot} can be

Algorithm 1 Weighted sum-rate maximization alg.

- 1: $a \leftarrow 0$ (set iteration number to zero)
- 2: $\{p_{s,0}^{i,k}, p_{r,0}^{i,k}, \zeta_{\text{sr},0}^{i,k}, \zeta_{\text{rd},0}^{i,k}\} \leftarrow$ feasible initialization
- 3: **repeat**
- 4: $a \leftarrow a + 1$
- 5: $\{p_s^{i,k}, p_r^{i,k}, \zeta_{\text{sr}}^{i,k}, \zeta_{\text{rd}}^{i,k}\} \leftarrow$ solve (33)
- 6: $\{p_{s,0}^{i,k}, p_{r,0}^{i,k}, \zeta_{\text{sr},0}^{i,k}, \zeta_{\text{rd},0}^{i,k}\} \leftarrow \{p_s^{i,k}, p_r^{i,k}, \zeta_{\text{sr}}^{i,k}, \zeta_{\text{rd}}^{i,k}\}$,
- 7: **until** a stable point, or maximum number of a reached
- 8: **return** $\{p_s^{i,k}, p_r^{i,k}\}$

expressed as [25]

$$P_{\text{tot}} = \sum_{i \in \mathbb{L}} P_s^i + P_r, \quad (34)$$

where

$$P_s^i := \frac{1}{\bar{\mu}_s^i} \sum_{k \in \mathbb{K}} \mathbb{E}\{\|x_s^{i,k}\|^2\} + P_{s,\text{zero}}^i,$$

$$P_r := \frac{1}{\bar{\mu}_r} \sum_{k \in \mathbb{K}} \mathbb{E}\{\|x_r^k\|^2\} + P_{r,\text{zero}} + P_{r,\text{FD}}.$$

The efficiency of the power amplifier and power dissipated by other circuit blocks at the transmitter chain of the i -th source node (relay) are respectively denoted by $\bar{\mu}_s^i$ ($\bar{\mu}_r$) and $P_{s,\text{zero}}^i$ ($P_{r,\text{zero}}$). $P_{r,\text{FD}}$ is the power required for SIC at the relay. By using the above definition, the energy efficiency maximization problem can be expressed as

$$\max_{\{p_s^{i,k}\}, \{p_r^{i,k}\}} \frac{\sum_{i \in \mathbb{L}} w_i \sum_{k \in \mathbb{K}} R^{i,k}(\mathbf{p})}{P_{\text{tot}}(\mathbf{p})} \quad (35a)$$

$$\text{s.t.} \quad (27b), (27c). \quad (35b)$$

The optimization problem can be reformulated in its epigraph form, similar to that of (28), as

$$\max_{\{p_s^{i,k}\}, \{p_r^{i,k}\}, \{\zeta_{\text{sr}}^{i,k}, \zeta_{\text{rd}}^{i,k}\}, t} \frac{t}{P_{\text{tot}}(\mathbf{p})} \quad (36a)$$

$$\text{s.t.} \quad (27b), (27c), (29b), (29c), (30b), (36b)$$

which shows a non-convex fractional structure. To solve the above problem, we propose a dual-loop iterative algorithm (Algorithm 2), employing the previously proposed SIA framework jointly with the Dinkelbach algorithm [14], proposed for iteratively solving different classes of fractional programs. Let us first select $p_{s,0}^{i,k}$ and $p_{r,0}^{i,k}$ as a feasible transmit power value at the i -th source node and relay, respectively. In the outer loop, we calculate the rate approximations $\bar{R}_{\text{sr}}^{i,k}$ and $\bar{R}_{\text{rd}}^{i,k}$ for the point of approximation $p_{s,0}^{i,k}$ and $p_{r,0}^{i,k}$, similar to the procedure presented in Algorithm 1. Please note that employing the aforementioned lower bounds leads to a concave-over-affine fractional program, which holds a pseudo convex structure. Consequently, the Dinkelbach algorithm [14] is employed in the inner loop by solving the optimization problem

$$\max_{\{p_s^{i,k}\}, \{p_r^{i,k}\}, \{\zeta_{\text{sr}}^{i,k}, \zeta_{\text{rd}}^{i,k}\}, t} t - \lambda P_{\text{tot}}(\mathbf{p}) \quad (37a)$$

$$\text{s.t.} \quad (27b), (27c), (33b), (33c), \quad (37b)$$

where λ is an auxiliary parameter introduced in the context of the Dinkelbach updates. For fixed $p_{s,0}^{i,k}$ and $p_{r,0}^{i,k}$, we iteratively solve for λ , $p_s^{i,k}$ and $p_r^{i,k}$. The value of λ can be then determined from

$$t - \lambda P_{\text{tot}} = 0. \quad (38)$$

Since Dinkelbach algorithm is applied to the concave-affine fractional problem, the iterates of Dinkelbach update converges to the optimum solution of the approximated problem [26, Section 3.2]. In the subsequent outer loop iteration, we update $p_{s,o}^{i,k}$ and $p_{r,o}^{i,k}$ in order to calculate the new rate approximations and solve the optimization problem until a stable point is reached. Algorithm 2 defines the algorithm procedure.

Algorithm 2 Energy efficiency maximization alg.

```

1:  $a \leftarrow 0$  (set iteration number to zero)
2:  $\{p_{s,o}^{i,k}, p_{r,o}^{i,k}, \zeta_{sr,0}^{i,k}, \zeta_{rd,0}^{i,k}\} \leftarrow$  feasible initialization
3: repeat
4:    $a \leftarrow a + 1$ 
5:    $\lambda = 0 \leftarrow$  Lambda initialization
6:   repeat
7:      $\{p_s^{i,k}, p_r^{i,k}, \zeta_{sr}^{i,k}, \zeta_{rd}^{i,k}\} \leftarrow$  solve (37)
8:      $\lambda \leftarrow$  solve (38)
9:   until a stable point is reached
10:   $\{p_{s,o}^{i,k}, p_{r,o}^{i,k}, \zeta_{sr,0}^{i,k}, \zeta_{rd,0}^{i,k}\} \leftarrow \{p_s^{i,k}, p_r^{i,k}, \zeta_{sr}^{i,k}, \zeta_{rd}^{i,k}\}$ 
11: until a stable point, or maximum number of  $a$  reached
12: return  $\{p_s^{i,k}, p_r^{i,k}\}$ 

```

C. Delivery Time Minimization

In this section, we address the joint sub-carrier and power allocation optimization problem to minimize the overall delivery time of an FD mMIMO relay system. Let us consider delivery time as the amount of time required to transmit D_i number of bits (size of a file) from the i -th source to the i -th destination. It can be defined as the ratio of the size of the file (amount of information D_i) required to be communicated between the i -th source-destination pair to the total achievable information rate of the i -th source-destination pair. Here, we formulate the optimization problem to minimize the overall delivery time for all the source-destination pairs.

The overall delivery time minimization problem can be defined as

$$\min_{\{p_s^{i,k}\}, \{p_r^{i,k}\}} \sum_{i \in \mathbb{L}} \frac{D_i}{\sum_{k \in \mathbb{K}} R^{i,k}(\mathbf{p})} \quad (39a)$$

$$\text{s.t.} \quad (27b), (27c). \quad (39b)$$

The above problem can be equivalently rewritten as

$$\min_{\{p_s^{i,k}\}, \{p_r^{i,k}\}, \{\zeta_{sr}^{i,k}, \zeta_{rd}^{i,k}\}, t} \sum_{i \in \mathbb{L}} \frac{D_i}{t_i} \quad (40a)$$

$$\text{s.t.} \quad \sum_{k \in \mathbb{K}} R_{sr}^{i,k}(\mathbf{p}, \zeta_{sr}^{i,k}) \geq t_i, \quad (40b)$$

$$\sum_{k \in \mathbb{K}} R_{rd}^{i,k}(\mathbf{p}, \zeta_{rd}^{i,k}) \geq t_i, \quad (40c)$$

$$(27b), (27c), (29b), (29c), (30b), (40d)$$

This optimization belongs to the class of smooth DC optimization problems similar to (27). After applying first order Taylor's approximation for the point of approximation $p_{s,o}^{i,k}$ and $p_{r,o}^{i,k}$, the approximated convex optimization can be reformu-

lated as

$$\max_{\{p_s^{i,k}\}, \{p_r^{i,k}\}, \{\zeta_{sr}^{i,k}, \zeta_{rd}^{i,k}\}, t} \sum_{i \in \mathbb{L}} \frac{D_i}{t_i} \quad (41a)$$

$$\text{s.t.} \quad \sum_{k \in \mathbb{K}} \bar{R}_{sr}^{i,k}(\mathbf{p}, \zeta_{sr}^{i,k}) \geq t_i, \quad (41b)$$

$$\sum_{k \in \mathbb{K}} \bar{R}_{rd}^{i,k}(\mathbf{p}, \zeta_{rd}^{i,k}) \geq t_i, \quad (41c)$$

$$(27b), (27c), (30b), \quad (41d)$$

which can be solved via standard convex numerical solvers. Similar to Algorithm 1 that follows SIA framework, the above procedure will be continued until convergence to a point that satisfies the KKT optimality conditions. Please see Algorithm 3 for the detailed algorithmic procedure.

Algorithm 3 Delivery time minimization alg.

```

1:  $a \leftarrow 0$  (set iteration number to zero)
2:  $\{p_{s,o}^{i,k}, p_{r,o}^{i,k}, \zeta_{sr,0}^{i,k}, \zeta_{rd,0}^{i,k}\} \leftarrow$  feasible initialization
3: repeat
4:    $a \leftarrow a + 1$ 
5:    $\{p_s^{i,k}, p_r^{i,k}, \zeta_{sr}^{i,k}, \zeta_{rd}^{i,k}\} \leftarrow$  solve (41)
6:    $\{p_{s,o}^{i,k}, p_{r,o}^{i,k}, \zeta_{sr,0}^{i,k}, \zeta_{rd,0}^{i,k}\} \leftarrow \{p_s^{i,k}, p_r^{i,k}, \zeta_{sr}^{i,k}, \zeta_{rd}^{i,k}\}$ 
7: until a stable point, or maximum number of  $a$  reached
8: return  $\{p_s^{i,k}, p_r^{i,k}, \zeta_{sr}^{i,k}, \zeta_{rd}^{i,k}\}$ 

```

IV. PERFORMANCE EVALUATION

In this section, using numerical simulations, we evaluate the performance of the proposed algorithms introduced in Section III-C for an FD mMIMO MC DF relay system with respect to different system parameters. We consider a relay communication setup where the distance between the sources/destinations to the FD mMIMO relay varying from 200m to 400m. The minimum distance between a source and a destination node is 400m. We adopt simulation system parameters from [27] and [28], which are chosen as in Table II. We consider our path loss model as a simplified path loss model in [29]. We consider that the relay employs OFDM as MC strategy. To provide fairness in resource allocation, the transmit power budgets are restricted to support the number of active sub-carriers, i.e., the transmit power budgets are factorized by k_t , where $k_t = \frac{|\mathbb{K}|}{|\mathbb{K}_{s,ys}|}$. For energy efficiency maximization problem, the power dissipated by circuit components other than power amplifier and power for SIC is also considered. The power dissipated by circuit blocks other than power amplifier at the transmitter chain of the i -th source node $P_{s,zero}^i$ and relay including SIC ($P_{r,zero} + P_{r,FD}$) are chosen as -20 dB and -16 dB, respectively. Here, the second order distortion coefficients at the transmitter (receiver) chains are not considered, i.e., $\kappa^{(2)} = \beta^{(2)} = 0$. For the delivery time minimization case, the file size (amount of information D_i) for each source-destination pair is chosen between 0 and 100 bits. All communication channels follow an uncorrelated Rayleigh flat fading model. The SI channel follows the Rician distribution as characterization reported in [20] with Rician coefficient K_r and the SI channel strength after SIC ρ_{si} . We

assume the covariance for the SI channel to be low rank as in [4]. Here, the rank of the covariance matrix of SI channel is chosen as 5. The overall system performance is then averaged over 100 channel realizations.

A. Benchmarks

For comparison, we consider different transmit/receive strategies at the relay for different system designs. The benchmarks considered for the numerical simulations are as follows.

- MRT/MRC: It represents the proposed Algorithms 1 to 3 employing MRT/MRC as relay transmit/receive strategy for the sum-rate maximization, energy efficiency maximization and delivery time minimization, respectively.
- MRT/MRC-SI-ZF: In addition to considering MRT/MRC as relay transmit/receive strategy, spatial suppression scheme (null-space projection [4]) for ZF the SI is employed at the transmit side of the relay. This allows to eliminate the receive distortion caused by the SI channel, since the transmit beams are projected to the null-space of the SI channel.
- ZF: The proposed Algorithms 1 to 3 employ ZF as its transmit/receive strategy at the relay.
- ZF-SI-ZF: In addition to considering ZF as the relay transmit/receive strategy, null-space projection scheme is also employed at the transmit side of the relay.

For the above-mentioned transmit strategies, we consider joint decoding and remapping (JC) strategy at the relay. It allows the relay system to decode the signal from one sub-carrier and forward it to the destination through another sub-carrier, thereby improving the performance of the system. We compare it to the per-carrier (PC) design, where the optimization constraints are considered for each sub-carrier individually. Moreover, the JC and PC designs for the above-mentioned transmit strategies are further classified as:

- OPT: It represents the proposed algorithms employing different transmit-receive strategies for both joint-carrier and per-carrier design, where the impact of imperfect CSI as well as the hardware distortions are taken into account.
- ND (non-distortion): It indicates the algorithms that do not consider the impact of hardware distortions in the design ($\kappa = 0$), i.e., a perfect hardware inaccuracy is assumed even though the system suffers from hardware distortions. It only considers the impact of imperfect CSI, similar to [15], [30], [31].
- HD: It indicates the scenarios when an HD mMIMO relay utilizes time division duplex to separate links between sources and destinations, similar to [32], [33].

B. Visualization

Figs. 2(a) to 2(f) illustrate the performance of the system for the sum-rate maximization algorithm with respect to different system parameters. In general, it can be observed that the algorithms employing ZF perform better compared the algorithms employed with MRT/MRC². However, the ZF strategy is more

²This is because in MRC/MRT scheme interference cannot be significantly reduced with a limited number of antennas (the random channel vectors are less pairwise orthogonal) and thus lowers the sum rate (compared to ZF scheme).

Carrier center frequency and system bandwidth	2.5 GHz and 5MHz
Number of sub-carriers $ \mathbb{K}_{e,y,s} $, and sub-carrier bandwidth	64 and 78kHz
Number of active sub-carriers $ \mathbb{K} $	10
Number of source-destination pairs $ \mathbb{L} $	3
Reference distance and path loss exponent	15m and 3.6
Efficiency of power amplifier at relay ($\bar{\mu}_r$) and source ($\bar{\mu}_k^t$)	0.39
Noise power at destination i and relay (σ_n^2)	-125dBm and -125dBm
Max. tx. power at the source ($P_{t,s,max}$) and relay ($P_{t,r,max}$)	22dBm and 37dBm
Number of antennas at the relay N	32
Hardware distortion coefficient $\kappa = \kappa^{(1)} = \beta^{(1)}$	-90dB
Covariance of the CSI estimation error $(\sigma_{e,ss}^k)^2 = (\sigma_{e,rd}^k)^2 = (\sigma_{e,sd}^k)^2 = (\sigma_{e,rs}^k)^2 \forall k \in \mathbb{K}$,	-150dB
SI channel strength ρ_{si} after SIC and Rician coefficient K_r	-50 dB and 10

TABLE II. DEFAULT SYSTEM PARAMETERS

complex (computationally expensive) compared to MRT/MRC as it involves inversion of matrices with large dimensions.

The performance of the Algorithm 1 in terms of sum-rate with respect to the hardware inaccuracies (κ) is shown in Fig. 2(a). As expected, the sum-rate decreases as hardware inaccuracies increases. It can be observed that a performance gain can be achieved by utilizing spatial suppression scheme (null-space projection) in addition to the transmit strategies. By transmitting along the null-space of the SI channel, the impact of receive distortion leading to residual SI (caused by the SI channel) can be eliminated. For MRT/MRC strategy, JC algorithms attain a notable gain in performance compared to its PC counterpart. Furthermore, the performance of ND algorithms is similar to that of the corresponding proposed OPT algorithms for small values of κ . However, as the value of κ increases, the performance of the ND algorithms degrades drastically compared to the OPT. As it can be observed, the achievable sum-rate of FD algorithms become less than that of the HD algorithms for higher values of κ . This implies that the impact of hardware distortion is more severer in FD systems compared to HD systems due to SI.

Fig. 2(b) depicts the system performance with respect to κ for different SI channel strength ($\rho_{si} = -30dB, -50dB$ and $-70dB$). It can be noticed that as the strength of the SI channel decreases (better SIC techniques), the performance of the FD systems is improved compared to its HD counterpart. It is interesting to observe that the HD mMIMO MC DF relay system shows better performance compared to the FD mMIMO MC DF relay system if sufficient SIC can not be achieved. For higher values of κ , the performance of the HD-ND algorithm degrades compared to the HD. This implies that even for HD mMIMO systems, consideration of hardware distortions into the design improves the system robustness and performance, especially in high hardware inaccuracies scenario.

Fig. 2(c) and 2(d) illustrate the performance of the algorithm Algorithm 1 for different values of receiver noise and channel estimation error, respectively. As expected, the sum-rate decreases as the receiver noise or channel estimation error increases. The performance of the system for both the parameters shows a similar trend. The OPT algorithm (ZF-SI-ZF) employing JC and ZF with SI suppression scheme performs better compared to all the other benchmarks. It is interesting to notice that for small values of receiver noise or channel estimation error, the OPT algorithm attains a better gain compared to its ND counterpart, and also employing

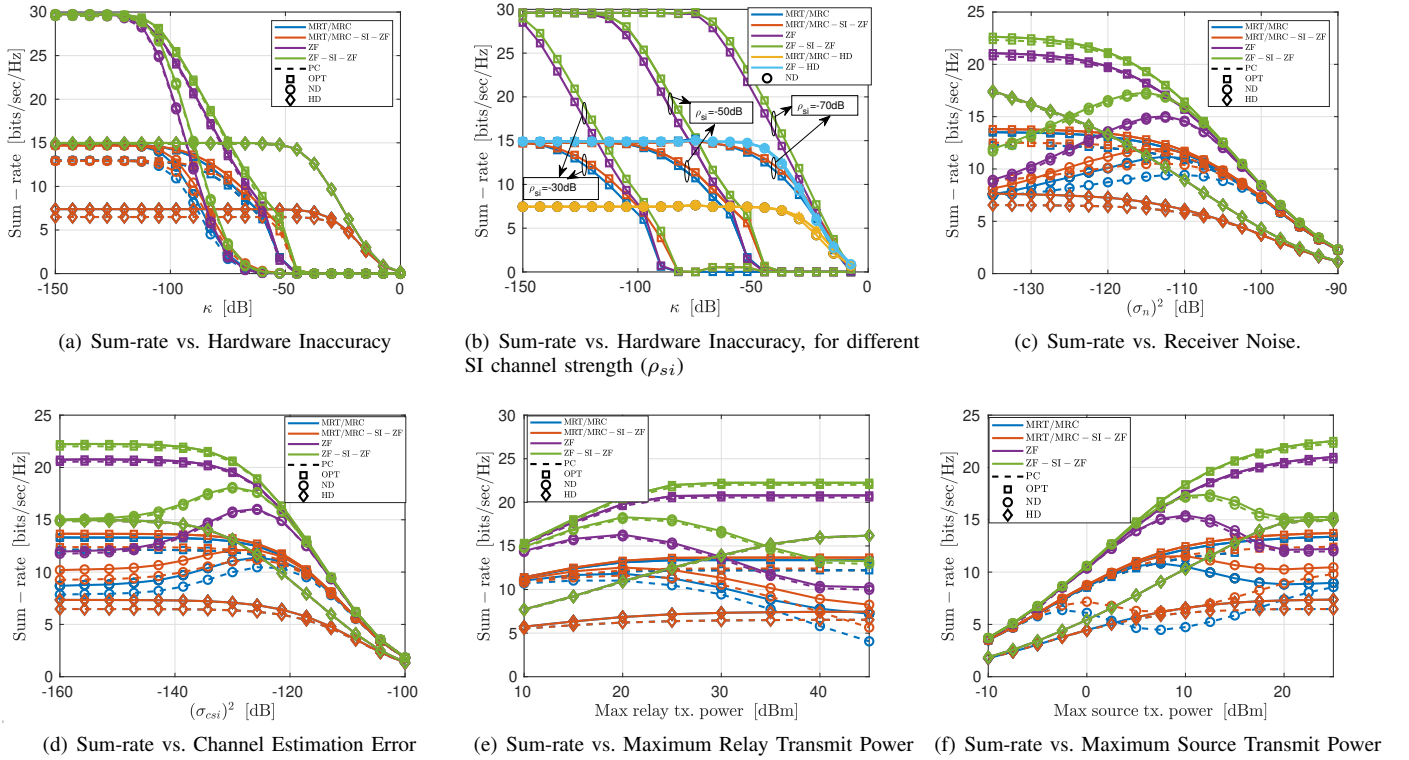


Fig. 2. Sum-rate for Different System Parameters

spatial suppression scheme provides a noticeable gain. This is due to the fact that for small values of receiver noise or channel estimation error, the impact of hardware distortion becomes dominant resulting in performance degradation of ND algorithm. In Figs. 2(e) and 2(f), the performance of the algorithm in terms of sum-rate for different values of relay and source transmit power is depicted, respectively. It can be noticed that when the maximum transmit power at the source/relay increases, the overall sum-rate also increases. It is interesting to observe that for high transmit power the ND algorithm performs worse compared to its OPT counterpart. This is because as the power increases, the hardware distortion becomes dominant at high transmit power scenario. The performance of the system in terms of sum-rate can be improved by considering hardware distortion and spatial suppression scheme, especially in high transmit power, low receiver noise or less estimation error scenarios.

In Figs. 3(a) to 3(c), the performance of the energy efficiency algorithm (Algorithm 2) for different system parameters is evaluated. In Fig. 3(a), the energy efficiency of the system degrades as the hardware inaccuracies increases, even for HD design. The proposed algorithm shows similar behavior as in the case of sum-rate maximization. Moreover, as the hardware inaccuracies increase, the HD algorithm performs better compared to the ND algorithm indicating that consideration of hardware distortion provides better gain for higher values of κ . In Fig. 3(c) and 3(b), the performance of the system in terms of energy efficiency is depicted with respect to the source transmit

power and receiver noise, respectively. The energy efficiency of the system degrades when the receiver noise increases. In contrast, as the source transmit power increases, the energy efficiency of the system increases. However, It is interesting to observe that for high transmit power and low noise values, the performance of the OPT algorithm in terms of energy efficiency is better compared to its ND counterpart since the hardware distortions become dominant. Another interesting observation is that the energy efficiency of the system becomes saturated at high transmit power budget. After a certain point, the optimum energy-efficient design does not consume much power when it degrades the energy efficiency of the system, i.e., only a small improvement in sum-rate is achieved with higher power requirements.

Figs. 4(a) to 4(d) illustrate the performance of the proposed delivery time minimization algorithm (Algorithm 3) for different system parameters. Similarly as in sum-rate and energy efficiency maximization case, it is observed that the ZF algorithms outperform the algorithms utilizing MRT/MRC. In Fig. 4(a), the performance of our proposed algorithm in terms of delivery time is evaluated for different values of transceiver accuracy. It can be observed that the delivery time increases as the transceiver inaccuracy increases. The OPT algorithms show better performance gain, i.e., less overall delivery time, compared to ND algorithms as the value of transceiver inaccuracies increases. This shows the significance of hardware-impairments aware design for an FD mMIMO MC relay system.

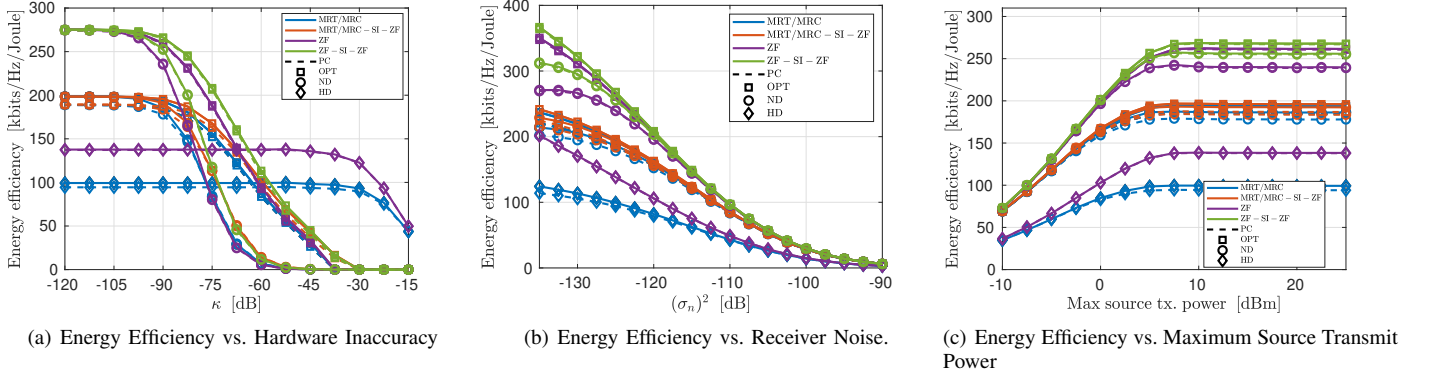


Fig. 3. Energy Efficiency for Different System Parameters

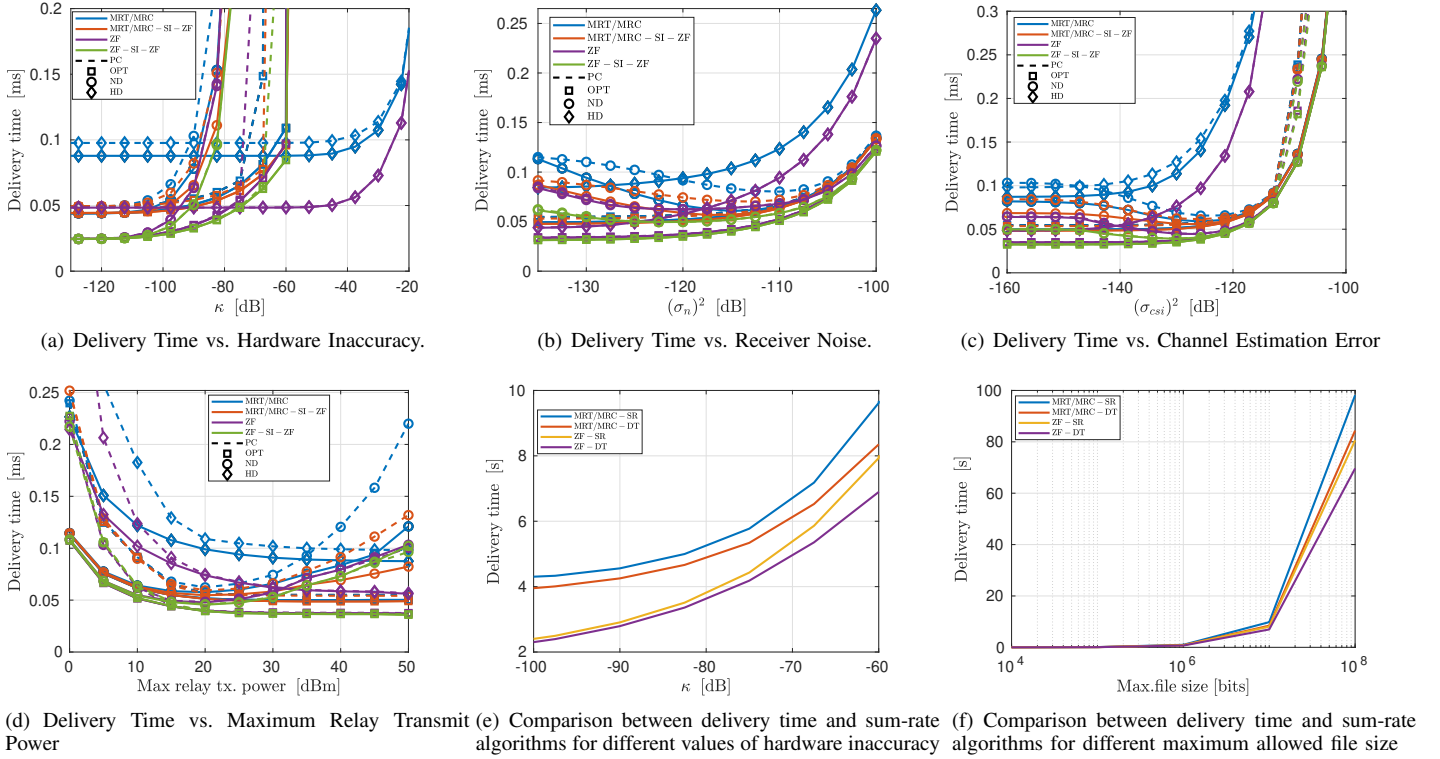


Fig. 4. Delivery Time for Different System Parameters

Figs. 4(b) and Fig. 4(c) illustrates the system performance in terms of delivery time with respect to different values of receiver noise and channel estimation error, respectively. As the receiver noise or channel estimation error increases, the overall delivery time also increases. Furthermore, we can observe that the proposed OPT algorithms outperform their respective ND and HD benchmarks. For small values of receiver noise variance or channel estimation error, the HD algorithms perform better than the ND algorithms. It is because, in high signal to interference plus noise (SINR) scenarios, the hardware distortions become dominant, thereby degrading the performance of ND algorithms. As the receiver noise variance

or channel estimation error increases, hardware distortions become less significant compared to these parameters resulting in better performance of ND algorithms compared to HD algorithms.

In Fig. 4(d) the performance of the proposed Algorithm 3 in terms of the delivery time for different values of relay transmit power is depicted. It can be noticed, as the maximum relay transmit power increases the overall delivery time decreases for all the algorithms except ND. For low transmit power values, the algorithms employing JC require less delivery time compared to its PC counterparts. This is because JC strategy has the flexibility to select the better channel on both the

link, i.e., source-relay and relay-destination for each source-destination pair, which becomes significant in low transmit power scenarios. As the transmit power increases, the overall delivery time for all the algorithms also decreases. However after a certain point, the performance of the ND algorithms degrade. It can also be observed that for a high transmit power scenario, the ND algorithm requires higher delivery time compared to HD and OPT algorithms. This is due to the fact that as transmit power increases the impact of hardware distortions also increases (due to SI), resulting in performance degradation of ND algorithms. This signifies the importance of consideration of the impact of hardware inaccuracies leading to ICL in an FD mMIMO MC relay system, especially for high transmit power, small channel estimation error and low noise scenarios. In case of delivery time minimization also, it is observed that the proposed algorithm (ZF-SI-ZF and MRT/MRC-SI-ZF) with JC outperforms all their respective benchmarks. This shows the benefit of considering hardware distortions, imperfect CSI, and utilizing JC and spatial suppression scheme in designing an FD mMIMO MC DF relay system for both transmit/receive strategies.

In Fig. 4(e), the performance of our proposed delivery time minimization algorithm is compared with the sum-rate maximization algorithm in terms of the delivery time for different values of transceiver accuracy. Here, the maximum file size (amount of information D_i) is chosen to be 10 Mbits. As it can be noticed, the delivery time algorithm performs better compared to the sum-rate algorithm, which implies that maximizing the throughput/sum-rate of the system does not necessarily minimize the overall delivery time. Fig. 4(f) shows the performance gain of delivery time algorithm compared to sum-rate algorithm for different maximum allowed file size (D_i). Here, the hardware distortion coefficients are chosen as $\kappa = \beta = -60\text{dB}$. It can be noticed that as the amount of information (D_i) to be communicated increases, the overall delivery time also increases. Furthermore, when the file size (D_i) is large, a significant gain in terms delivery time can be achieved by utilizing the delivery time minimization algorithm in comparison with the sum-rate maximization algorithm.

C. Second Order Distortion

In this section, we evaluate the performance of the proposed algorithm Algorithm 1 for different system parameters by taking into account the second-order statistics of hardware distortions. For this simulations, the following values are used to define the default setup: $|\mathbb{K}| = 8$, $|\mathbb{L}| = 3$, $P_{t,r,max} = -10\text{dB}$, $P_{t,s,max} = 0\text{dB}$, $\bar{\mu}_r = \bar{\mu}_s^i = 0.99$, (channel strength) $\rho_{sr} = \rho_{rd} = -10\text{dB}$, $\rho_{sd} = -40\text{dB}$, $\rho_{si} = 0\text{dB}$, $\kappa^{(1)} = \beta^{(1)} = -50\text{dB}$, $\kappa^{(2)} = \beta^{(2)} = -40\text{dB}$ and receiver noise $\sigma_n = \sigma_d^i = -40\text{dB}$. We also assume a perfect CSI is available. The curves MRT/MRC – with $\kappa^{(2)}$ and MRT/MRC ($\kappa^{(2)} = 0$) represent the algorithms with and without consideration of second order hardware distortions, respectively. The MRT/MRC – ND curve represents the algorithm that does not consider the hardware distortion ($\kappa^{(1)} = \beta^{(1)} = \kappa^{(2)} = \beta^{(2)} = 0$).

Fig. 5(a) shows the performance for the algorithm Algorithm 1 with respect to the second-order distortion coefficients ($\kappa^{(2)} = \beta^{(2)}$) for different values of first order distortion coefficient ($\kappa^{(1)} = \beta^{(1)}$). It can be observed that the performance of the proposed algorithm degrades as the value of $\kappa^{(2)}$ increases. For smaller values of $\kappa^{(1)}$, the difference in performance between MRT/MRC – with $\kappa^{(2)}$ and MRT/MRC ($\kappa^{(2)} = 0$) increases. This because the second order hardware distortions become dominant for smaller values of $\kappa^{(1)}$. In Fig. 5(b), the performance of the algorithm is evaluated with respect to the relay and destination receiver noise for different values of $\kappa^{(2)}$. The performance of the proposed algorithm reduces as the receiver noise increases. It can be observed that after a certain point, the performance of MRT/MRC – ND degrades as the noise values decreases. This is because for small values of receiver noise the hardware distortion becomes dominant, resulting in reduction of performance of the MRT/MRC – ND algorithm that does not consider or ignores the hardware distortions present in the system. Similarly as the values of receiver noise decreases, the performance of MRT/MRC ($\kappa^{(2)} = 0$) degrades compared to MRT/MRC – with $\kappa^{(2)}$. Since the MRT/MRC ($\kappa^{(2)} = 0$) algorithm ignores the second order hardware distortion in a hardware distortion dominant scenario. Fig. 5(a) and Fig. 5(b) demonstrate that with consideration of second order hardware in the design a noticeable gain can be achieved, especially for smaller values of receiver noise and first order hardware distortion coefficient ($\kappa^{(1)}$).

D. Convergence

In Fig. 6(a) the average convergence behavior of our proposed algorithm Algorithm 1 with equal power initialization for different values of hardware inaccuracy κ dB is depicted. The relay employs MRT/MRC as its transmit/receive strategy. The simulation setup is similar to that in the previous section. Here, the second-order distortions are not considered. It can be noticed that the algorithm converges within 10-25 iterations. As expected, it can be seen that the objective has a higher value for smaller hardware inaccuracy. However, 6(b) illustrates the optimality gap of our algorithm. During numerical simulations, an increase in the optimality gap is observed when the higher hardware inaccuracies increase. This is expected, as larger κ leads to a more complex problem structure.

V. CONCLUSION

In this paper, we investigated the joint sub-carrier and power allocation problem for an FD mMIMO MC DF relay system that serves multiple single-antenna HD source-destination pairs. We modeled the operation of the system by jointly considering the impact of hardware distortion leading to residual SI and ICL, and imperfect CSI. An iterative algorithm that follows the SIA framework is proposed for sum-rate maximization and delivery time minimization problem, which converges to the point that satisfies the KKT conditions. Using numerical simulations, it is noticed that utilizing JC and spatial suppression scheme provides additional performance gain for both MRT/MRC and ZF strategies. A notable gain in terms

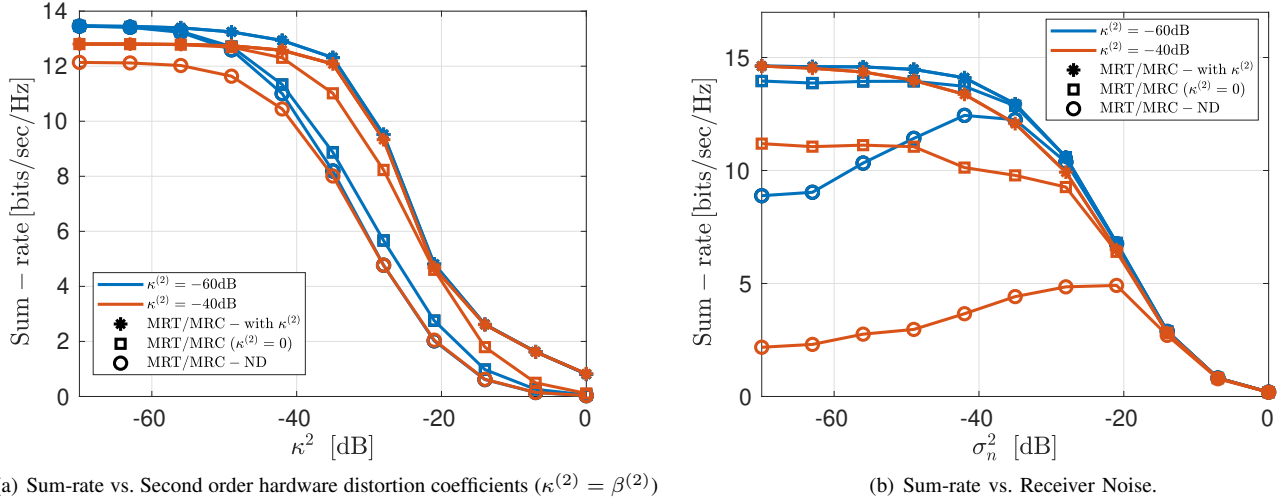


Fig. 5. Sum-rate for different system parameters considering second order hardware distortions

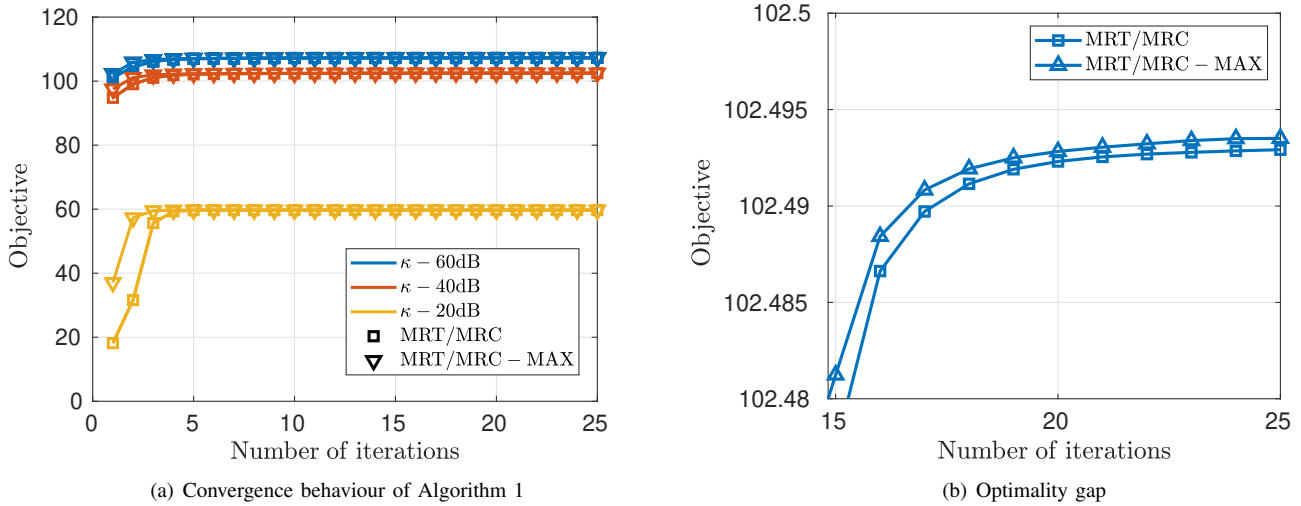


Fig. 6. Convergence behaviour of Algorithm 1

of delivery time is achieved when compared with the sum-rate maximization algorithm, shows the benefit of considering delivery time as an objective. Significance of distortion-aware design for an FD mMIMO MC DF relay system is observed, especially for high SINR scenarios.

VI. ACKNOWLEDGMENT

The authors would like to thank Dr.-Ing. habil. Gholamreza Alirezaei for valuable discussions.

APPENDIX A PROOF OF LEMMA II.1

The time domain statistical independence $e_{t,l}(t) \perp v_l(t)$ and $e_{t,l}(t) \perp e_{t,l'}(t)$, and the linear nature of the transformation (20) are also applicable to the statistical independence properties at

the transformed unitary domain. Similarly, the Gaussian and zero-mean properties for $e_{t,l}^k$ becomes a linearly weighted sum of the zero-mean Gaussian values $e_{t,l}(mT_s)$. The variance of $e_{t,l}^k$ can hence be obtained as

$$\begin{aligned}
 \mathbb{E} \left\{ |e_{t,l}^k|^2 \right\} &= \mathbb{E} \left\{ \left(\sum_{m=0}^{N-1} e_{t,l}(mT_s) q_{k,m}^* \right) \times \left(\sum_{n=0}^{N-1} e_{t,l}^*(nT_s) q_{k,n} \right) \right\} \\
 &= \sum_{m=0}^{N-1} \sum_{n=0}^{N-1} \mathbb{E} \{ e_{t,l}(mT_s) e_{t,l}^*(nT_s) \} q_{k,m} q_{k,n}^* \\
 &= \sum_{m=0}^{N-1} \mathbb{E} \{ e_{t,l}(mT_s) e_{t,l}^*(mT_s) \} q_{k,m} q_{k,m}^* \quad (e_{t,l}(t) \perp e_{t,l}(t')) \\
 &= \kappa \left(\mathbb{E} \{ |v_l(t)|^2 \}, \kappa_l^{(1)}, \kappa_l^{(2)} \right) / K \quad (\text{From (17) and } \sum_{m=0}^{N-1} q_{k,m} q_{k,m}^* = 1)
 \end{aligned}$$

$$= \kappa \left(\sum_{m=1}^K \mathbb{E} \{ |v_l^m|^2 \}, \kappa_l^{(1)}, \kappa_l^{(2)} \right) / K. \quad (\text{Parseval's theorem}).$$

Similarly, the receiver characterization can be proved.

REFERENCES

- [1] V. Radhakrishnan, O. Taghizadeh, and R. Mathar, "Resource Allocation for Full-Duplex MU-mMIMO Relaying: A Delivery Time Minimization Approach," in *24th International ITG Workshop on Smart Antennas (WSA 2020)*, Hamburg, Germany, Feb. 2020.
- [2] V. Wong, "Key technologies for 5G wireless systems" *Cambridge university press*, 2017
- [3] H. Q. Ngo, E. G. Larsson, and T. L. Marzetta, "Energy and spectral efficiency of very large multiuser mimo systems," *IEEE Transactions on Communications*, vol. 61, no. 4, pp. 1436–1449, April 2013.
- [4] T. Riihonen, S. Werner, and R. Wichman, "Mitigation of loopback self-interference in full-duplex mimo relays," *IEEE Transactions on Signal Processing*, vol. 59, no. 12, pp. 5983–5993, Dec 2011.
- [5] H. Q. Ngo, H. A. Suraweera, M. Matthaiou, and E. G. Larsson, "Multi-pair full-duplex relaying with massive arrays and linear processing," *IEEE Journal on Selected Areas in Communications*, vol. 32, no. 9, pp. 1721–1737, Sep. 2014.
- [6] y. li, P. Fan, A. Leukhin, and L. Liu, "On the spectral and energy efficiency of full-duplex small cell wireless systems with massive mimo," *IEEE Transactions on Vehicular Technology*, vol. 66, Jan 2016.
- [7] H. A. Suraweera, H. Q. Ngo, T. Q. Duong, C. Yuen, and E. G. Larsson, "Multi-pair amplify-and-forward relaying with very large antenna arrays," in *2013 IEEE International Conference on Communications (ICC)*, June 2013, pp. 4635–4640.
- [8] S. Wang, Y. Liu, W. Zhang, and H. Zhang, "Achievable rates of full-duplex massive mimo relay systems over rician fading channels," *IEEE Transactions on Vehicular Technology*, vol. 66, no. 11, Nov 2017.
- [9] W. Xie, X. Xia, Y. Xu, K. Xu, and Y. Wang, "Massive mimo full-duplex relaying with hardware impairments," *Journal of Communications and Networks*, vol. 19, no. 4, pp. 351–362, August 2017.
- [10] X. Xia, D. Zhang, K. Xu, W. Ma, and Y. Xu, "Hardware impairments aware transceiver for full-duplex massive mimo relaying," *IEEE Transactions on Signal Processing*, vol. 63, no. 24, pp. 6565–6580, Dec 2015.
- [11] B. P. Day, A. R. Margetts, D. W. Bliss, and P. Schniter, "Full-Duplex MIMO Relaying: Achievable Rates Under Limited Dynamic Range," in *IEEE Journal on Selected Areas in Communications*, 2012.
- [12] O. Taghizadeh, V. Radhakrishnan, A. C. Cirik, R. Mathar, and L. Lampe, "Hardware Impairments Aware Transceiver Design for Bidirectional Full-Duplex MIMO OFDM Systems," *IEEE Transactions on Vehicular Technology*, vol. 67, no. 8, pp. 7450–7464, Aug 2018.
- [13] A. Papazafeiropoulos, B. Clerckx, and T. Ratnarajah, "Rate-splitting to mitigate residual transceiver hardware impairments in massive mimo systems," *IEEE Transactions on Vehicular Technology*, vol. 66, no. 9, pp. 8196–8211, Sep. 2017.
- [14] W. Dinkelbach, "On nonlinear fractional programming," *Management Science*, vol. 13, no. 7, pp. 492–498, 1967.
- [15] A. C. Cirik, Y. Rong, and Y. Hua, "Achievable rates of full-duplex mimo radios in fast fading channels with imperfect channel estimation," *IEEE Transactions on Signal Processing*, vol. 62, pp. 3874–3886, Aug 2014.
- [16] B. P. Day, D. W. Bliss, A. R. Margetts, and P. Schniter, "Full-duplex bidirectional MIMO: Achievable rates under limited dynamic range," in *2011 Conference Record of the Forty Fifth Asilomar Conference on Signals, Systems and Computers*, Nov 2011, pp. 1386–1390.
- [17] W. Namgoong, "Modeling and analysis of nonlinearities and mismatches in ac-coupled direct-conversion receiver," *IEEE Transactions on Wireless Communications*, vol. 4, no. 1, pp. 163–173, Jan 2005.
- [18] G. Santella and F. Mazzenga, "A hybrid analytical-simulation procedure for performance evaluation in m-qam-ofdm schemes in presence of nonlinear distortions," *IEEE Transactions on Vehicular Technology*, vol. 47, no. 1, pp. 142–151, Feb 1998.
- [19] H. Suzuki, T. V. A. Tran, I. B. Collings, G. Daniels, and M. Hedley, "Transmitter noise effect on the performance of a mimo-ofdm hardware implementation achieving improved coverage," *IEEE Journal on Selected Areas in Communications*, vol. 26, no. 6, August 2008.
- [20] M. Duarte, C. Dick, and A. Sabharwal, "Experiment-Driven Characterization of Full-Duplex Wireless Systems," *IEEE Transactions on Wireless Communications*, vol. 11, pp. 4296–4307, December 2012.
- [21] O. Taghizadeh, A. C. Cirik and R. Mathar, "Hardware Impairments Aware Transceiver Design for Full-Duplex Amplify-and-Forward MIMO Relaying," in *IEEE Transactions on Wireless Communications*, vol. 17, no. 3, pp. 1644–1659, March 2018.
- [22] V. Radhakrishnan, O. Taghizadeh, and R. Mathar, "Asymptotic Rate Analysis for Impairments-Aware Multi-Carrier FD Massive MIMO Relay Networks utilizing MRT/MRC Strategy," in *arXiv (preprint)*, Nov. 2020.
- [23] B. R. Marks and G. P. Wright, "Technical note—a general inner approximation algorithm for nonconvex mathematical programs," *Operations Research*, vol. 26, no. 4, pp. 681–683, 1978.
- [24] S. Boyd and L. Vandenberghe, *Convex Optimization*. New York, NY, USA: Cambridge University Press, 2004.
- [25] O. Taghizadeh, P. Neuhaus, R. Mathar and G. Fettweis, "Secrecy Energy Efficiency of MIMOME Wiretap Channels With Full-Duplex Jamming," in *IEEE Transactions on Communications*, vol. 67, no. 8, pp. 5588–5603, Aug. 2019.
- [26] A. Zappone and E. Jorswieck, *Energy Efficiency in Wireless Networks via Fractional Programming Theory*. Hanover, MA, USA: Now Publishers Inc., 2015.
- [27] 3GPP, "Evolved Universal Terrestrial Radio Access (E-UTRA); Further advancements for E-UTRA physical layer aspects," Technical report (TR) 36.814, March 2010, version 2.0.0.
- [28] Y. Sun, D. W. K. Ng, J. Zhu, and R. Schober, "Robust and secure resource allocation for full-duplex miso multicarrier noma systems," *IEEE Transactions on Communications*, vol. 66, no. 9, Sep. 2018.
- [29] A. Goldsmith, *Wireless Communications*. Cambridge University Press, 2005.
- [30] D. W. K. Ng, E. S. Lo and R. Schober, "Energy-Efficient Resource Allocation in OFDMA Systems with Large Numbers of Base Station Antennas," *IEEE Transactions on Wireless Communications*, vol. 11, no. 9, pp. 3292–3304, September 2012.
- [31] O. Taghizadeh, J. Zhang, and M. Haardt "Transmit beamforming aided amplify-and-forward MIMO full-duplex relaying with limited dynamic range," *Signal Processing 127 (2016): 266-281*.
- [32] J. Chen, X. Chen, W. H. Gerstacker, and D. W. K. Ng, "Resource Allocation for a Massive MIMO Relay Aided Secure Communication," in *IEEE Transactions on Information Forensics and Security*, vol. 11, no. 8, pp. 1700–1711, 2016.
- [33] H. Gao, T. Lv, X. Su, H. Yang, and J. M. Cioffi, "Energy-Efficient Resource Allocation for Massive MIMO Amplify-and-Forward Relay Systems," in *IEEE Access*, vol. 4, pp. 2771–2787, 2016.